AD-A164 164 DAMAGE MODELS FOR DELAMINATION AND TRANSVERSE FRACTURE IN FIBROUS COMPOSI.. (U) TEXAS A AND M UNIV COLLEGE STATION MECHANICS AND MATERIALS RE.. 1/1

UNCLASSIFIED R A SCHAPERY ET AL. MAY 85 MM-5034-85-8 F/G 11/5 NL

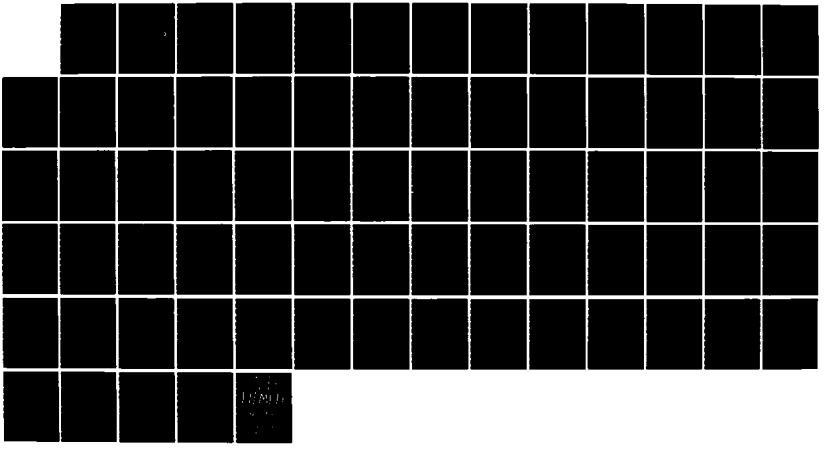

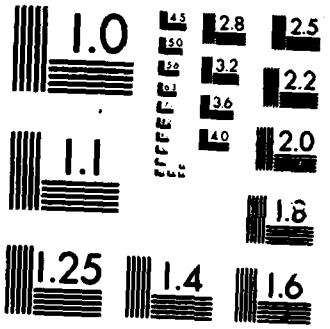

Mechanics and Materials Center
TEXAS A&M UNIVERSITY
College Station, Texas

DAMAGE MODELS FOR DELAMINATION AND TRANSVERSE FRACTURE

ANNUAL TECHNICAL REPORT

R.A. Schapery

J.R. Weatherby

R.D. Tonda

AIR FORCE OFFICE OF SCIENTIFIC RESEARCH

OFFICE OF AEROSPACE RESEARCH

UNITED STATES AIR FORCE

GRANT NO. AFOSR-84-0068

MM 5034-85-8

MAY 1985

unclassified

SECURITY CLASSIFICATION OF THIS PAGE

REPORT DOCUMENTATION PAGE

1a. REPORT SECURITY CLASSIFICATION: Unclassified	1b. RESTRICTIVE MARKINGS
2a. SECURITY CLASSIFICATION AUTHORITY	3. DISTRIBUTION/AVAILABILITY OF REPORT: unlimited Approved for public release; distribution unlimited.
2b. DECLASSIFICATION/DOWNGRADING SCHEDULE	
4. PERFORMING ORGANIZATION REPORT NUMBER(S): MM 5034-85-8	5. MONITORING ORGANIZATION REPORT NUMBER(S): AFOSR-TR- 85-1226
6a. NAME OF PERFORMING ORGANIZATION: Mechanics and Materials Center, Texas A&M University; 6b. OFFICE SYMBOL (If applicable):	7a. NAME OF MONITORING ORGANIZATION: AFOSR/NA
6c. ADDRESS (City, State and ZIP Code): College Station, TX 77843	7b. ADDRESS (City, State and ZIP Code): Building 410, Bolling AFB, DC 20332-6448
8a. NAME OF FUNDING/SPONSORING ORGANIZATION: AFOSR/NA; 8b. OFFICE SYMBOL (If applicable): NA AFOSR	9. PROCUREMENT INSTRUMENT IDENTIFICATION NUMBER: Grant No. AFOSR-84-0068
8c. ADDRESS (City, State and ZIP Code): Building 410, Bolling AFB, DC 20332-6448	10. SOURCE OF FUNDING NOS.

PROGRAM ELEMENT NO.	PROJECT NO.	TASK NO.	WORK UNIT NO.
61102F	2302	B2	

11. TITLE (Include Security Classification): Damage Models for Delamination and Transverse Fracture in Fibrous Composites

12. PERSONAL AUTHOR(S): R.A. Schapery, J.R. Weatherby, R.D. Tonda

13a. TYPE OF REPORT	13b. TIME COVERED	14. DATE OF REPORT (Yr., Mo., Day)	15. PAGE COUNT
Annual	FROM 2/15/84 TO 2/14/85	May 1985	29 + Appendix

16. SUPPLEMENTARY NOTATION

17. COSATI CODES		
FIELD	GROUP	SUB. GR.

18. SUBJECT TERMS (Continue on reverse if necessary and identify by block number): Composites; Damage; Delamination; Fracture of Composites; Fiber-Reinforced Plastic

19. ABSTRACT (Continue on reverse if necessary and identify by block number)

Theoretical and experimental work on the deformation and fracture of fibrous composites with distributed damage is described. Emphasis is on establishing the existence of potentials analogous to strain energy and on using these so-called work potentials in fracture studies. The difference between loading and unloading behavior is accounted for by using one work potential for changing damage (loading) and another for constant damage (unloading). First, using work potentials in a finite element representation, a new method for predicting crack growth is described which is believed to be applicable to many different materials. The results confirm the previously predicted path independence of the J integral for a crack in a continuum with distributed damage; the damage is modelled in this initial study using deformation plasticity theory for loading and elasticity theory for unloading. Described next are investigations of flat rectangular bar specimens and thin-walled tubes under axial and torsional loading. The limited amount of experimental data presently available on angle-ply laminates confirms the existence of a potential even when there are large increases in microcracking.

20. DISTRIBUTION/AVAILABILITY OF ABSTRACT	21. ABSTRACT SECURITY CLASSIFICATION
UNCLASSIFIED/UNLIMITED ☒ SAME AS RPT. ☐ DTIC USERS ☐	unclassified

22a. NAME OF RESPONSIBLE INDIVIDUAL	22b. TELEPHONE NUMBER (Include Area Code)	22c. OFFICE SYMBOL
Major David A. Glasgow	(202) 767-4987	AFOSR NA

DD FORM 1473, 83 APR EDITION OF 1 JAN 73 IS OBSOLETE.

unclassified

SECURITY CLASSIFICATION OF THIS PAGE

TABLE OF CONTENTS

1. RESEARCH OBJECTIVES

The overall objective of the research is to develop and verify mathematical models of delamination and transverse fracture which account for local (crack tip) and global damage distributions. One specific objective is to demonstrate theoretically and experimentally that "work potentials" (which are analogous to strain energy) exist for composites with constant and changing damage and with viscoelastic behavior. The second objective is to develop and verify methods of analysis for predicting crack growth in elastic and viscoelastic composites with distributed damage; whenever they are justified, work potentials will be used to characterize material behavior in order to simplify fracture analysis.

2. STATUS OF THE RESEARCH

2.1 Introduction

Methods of deformation and fracture characterization and prediction are simplified when strain energy-like potentials based on mechanical work can be used, as described in the publications in the Appendix. With these so-called work potentials, important theoretical and experimental methods using the J integral and energy release rate (originally developed for fracture of elastic media and fracture initiation in metals with plastic deformations) may be extended to fracture initiation and crack propagation in monolithic and composite materials. In Section 2.2, graduate student Randy Weatherby describes a new finite element model for analyzing crack growth in materials which are characterized by work potentials. It is believed that both the use of the "failure zone" in a finite element model

and the study of path independence of the J integral with crack propagation are new. Graduate student Richard Tonda describes in Section 2.3 his work on determining work potentials for a graphite/epoxy composite using unidirectional bars and circular tubes. The computer, computer programs, and reduced data were all lost in a fire on December 31, 1984. This study has been discontinued for now; but it probably will be restarted early this coming Fall. In place of this work, we have begun a study of flat angle-ply laminated bars under combined axial and torsional loading, as described in Section 2.4. A third graduate student, Mark Lamborn, recently joined the project, and he has contributed to the study described in Section 2.4. Preliminary data confirm the existence of a work potential. Also, early results indicate that the tests of flat bars with axial and torsional loading will be useful for Mode III delamination investigations.

2.2 Analysis of Crack Growth in Damaged Media Using a Generalized J-Integral

The purpose of this research is to develop and study analytical methods for use in nonlinear fracture problems with distributed damage. We feel that these methods can be applied to a wide variety of materials including metals, polymers, and fibrous composites. Our current approach is to deal with crack advance purely from a mechanics viewpoint, given certain characteristics of the zone of failing material at the crack tip.

A central idea in the theory of fracture which we follow is that the stresses and strains in the continuum are bounded rather than singular at the crack tip. This condition is met by the introduction of a "failure zone" at the end of an advancing crack. The failure zone is a thin layer of highly strained and damaged material which is usually surrounded by inelastic material (see Figure 1). The failure zone can be represented in a finite element model as a nonlinear foundation which extends ahead of the crack. This foundation is divided into discrete elements, which we call failure zone elements, and a relationship between the tractions acting on the crack surface and the opening displacement is specified. The traction-displacement function is defined so that after a certain amount of separation between the crack faces the surface tractions vanish and the crack increases in length. Similar techniques have been used previously in modeling fracture of concrete, adhesive joints, and composites [1,2]. In these cases, however, the continuum surrounding the failure zone is assumed to be linearly elastic, whereas we are presently considering problems in which the surrounding continuum is a rate independent, inelastic material.

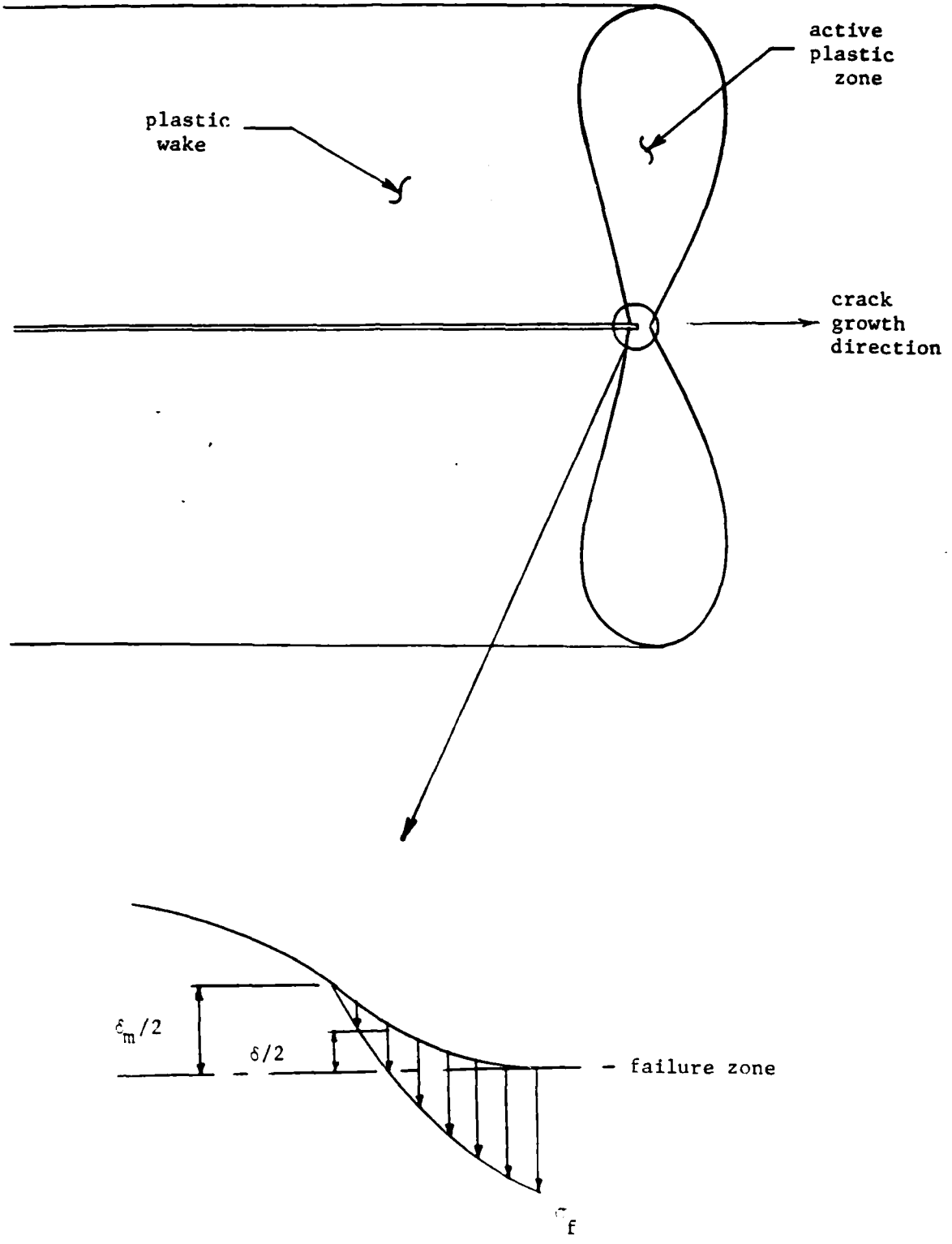

Figure 1. Crack Tip Region

Under certain conditions (which will be stated shortly) it can be shown that there is a path independent J-integral [3], and it is equal to the total work input per unit area to a ligament at the trailing edge of the failure zone. First consider a line integral defined by:

$$J_B = \int_B (\Phi n_1 - T_i \frac{\partial u_i}{\partial x_1}) \, ds \qquad (1)$$

where,

B = the contour of integration

Φ = potential function analogous to strain energy density.

T_i = traction vector acting on B.

u_i = displacement vector.

n_1 = x_1-component of the unit vector normal to B.

As an example, using $\mathscr{L}$ to denote the value of (1) for the closed contour in Figure 2, and expressing it as the sum of contributions from each segment of the total path, we have, *using clockwise integration*,

$$\mathscr{L} = J_{AB} + J_{BC} + J_{CD} + J_{DE} + J_{EF} + J_{FG} + J_{GH} + J_{HI} + J_{IJ} + J_{JA} \qquad (2)$$

For an opening mode crack, symmetry can be used to give:

$$\mathscr{L} = 2 \, (J_{AB} + J_{BC} + J_{CD} + J_{DE} + J_{JA}) \qquad (3)$$

For the material model we use, $\mathscr{L}$ will be zero when evaluated around any closed contour, B, provided that inside of B, $\tau_{max}(x,y) = \tau_{max}(y)$ for points where $\tau > \tau_{max}$ if $\tau_{max} > \tau_o$. Here, $\tau(x,y)$ is the octahedral shear stress, τ_o is the value of τ at which appreciable plastic deformation occurs, and τ_{max} is the maximum value of τ seen by a material point over the entire history of loading. It is assumed that the regions which

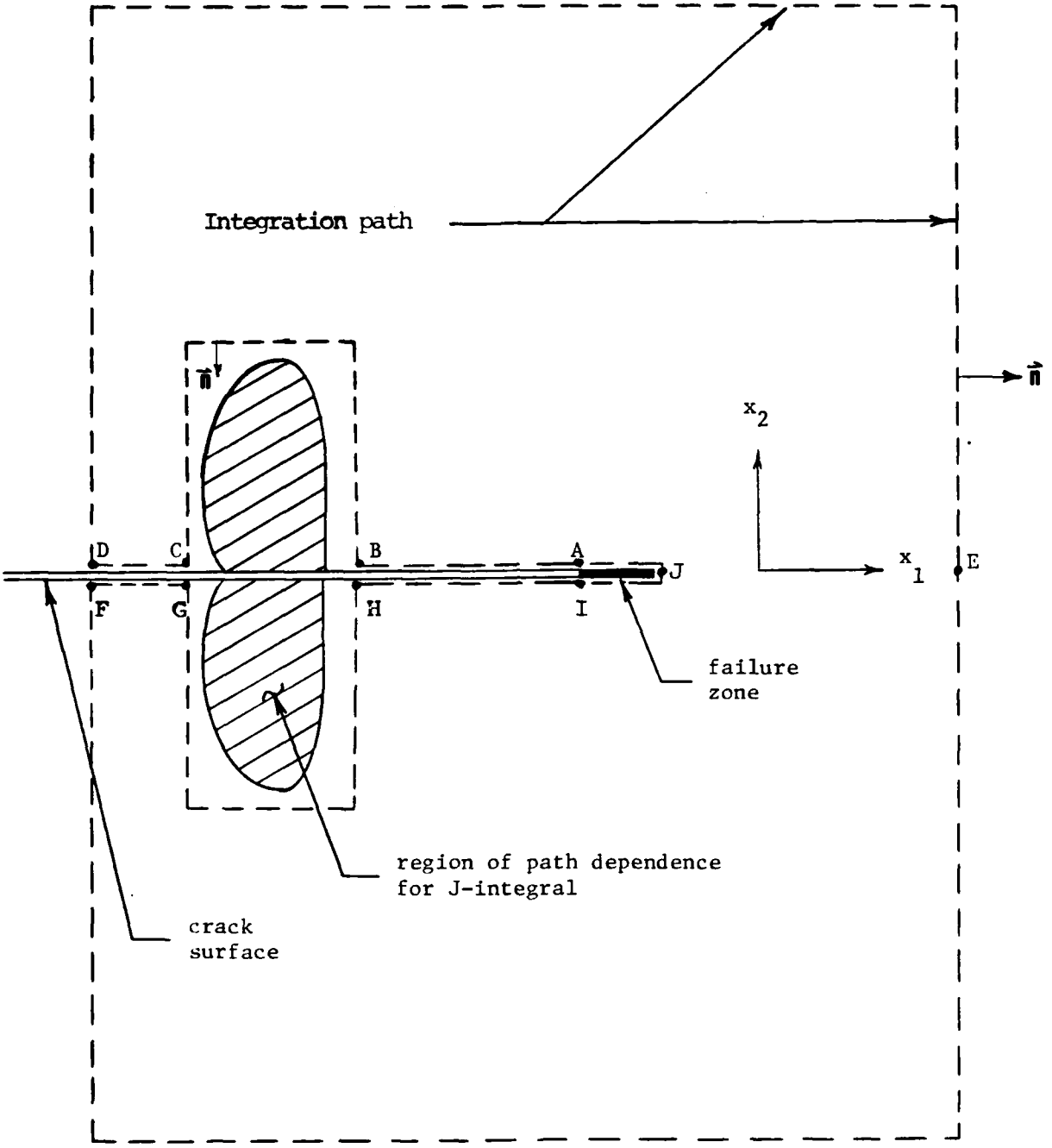

Figure 2. Contour Path for J-Integral

violate the $\mathscr{L}$=0 condition have been excluded from the interior of B; Equation (3) becomes, after setting $\mathscr{L}$= 0,

$$2\ (J_{AB} + J_{BC} + J_{CD} + J_{DE}) = -2J_{JA} \tag{4}$$

Further, we note that $n_1 = 0$ and $T_i = 0$ on segments AB and CD. When tractions in the failure zone are given as a function of displacements, it can be shown that [4],

$$2J_{JA} = -2\Gamma \tag{5}$$

where 2Γ is the work per unit area done to a ligament at the left end of the failure zone. These observations allow (4) to be rewritten as:

$$2\ (J_{BC} + J_{DE}) = 2\Gamma \tag{6}$$

In the remainder of this report, when we give a value for the J-integral, we are referring to the value of the line integral in Eq. (1), but integrated only over an open contour with end points at the left end of the failure zone (in the case of a right moving crack tip). For example, in Fig. 2 the value of J to which we refer is $2\ (J_{BC} + J_{DE})$.

In order to verify by an example that the necessary conditions for path independence of J are satisfied after crack advance, we analyzed the small scale yielding problem in an isotropic material using the finite element method. This problem also serves to demonstrate the usefulness of the failure zone element in determining crack growth. By definition, in the small scale yielding problem, the plastic zone size is small when compared to the crack length and the distance to the nearest boundary. The displacement field far away from the crack tip is specified to be of the form found for a crack in a linearly elastic body ie.,

$$u_i = K_I \sqrt{r} \quad f_i(\theta) \tag{7}$$

Figure 3 shows the dimensions and boundary conditions used in the finite element model, and Figs. 4 and 5 give the continuum and failure zone constitutive functions, respectively. Substructuring is used to condense out the degrees of freedom in the linearly elastic region, leaving only the nodes associated with the elements appearing in Figure 6. All continuum elements have eight nodes, and displacement continuity between incompatible elements (i.e., where 3 elements share a common boundary as shown in Fig. 6) is enforced approximately by a penalty method. A J_2 deformation theory of plasticity with elastic unloading is taken as the material model for the continuum. Figs. 4 and 5 show the various material constants which are required; these include parameters describing the uniaxial stress-strain curve for the continuum and the traction-displacement relationship for the failure zone. For simplicity, it is assumed that the traction-displacement curve is independent of the amount of crack advance (i.e., the work of fracture, 2Γ, and crack tip opening displacement are held constant). Loading is accomplished by increasing the stress intensity factor. This is not done directly; rather, a modified Riks' algorithm [5] is used in order to get past limit points due to the finite element approximation which sometimes appear. As the stress intensity factor increases, a plastic zone forms around the crack tip, and the failure zone elements separate to give crack advance. Figure 6 shows the area where significant plastic deformation has taken place after the crack has grown some distance. The term "active plastic zone" refers to the material points currently at yield, and "plastic wake" refers to the points which have yielded and then unloaded as the crack tip passed by.

A plot of the dimensionless elastic "energy release rate" as a function

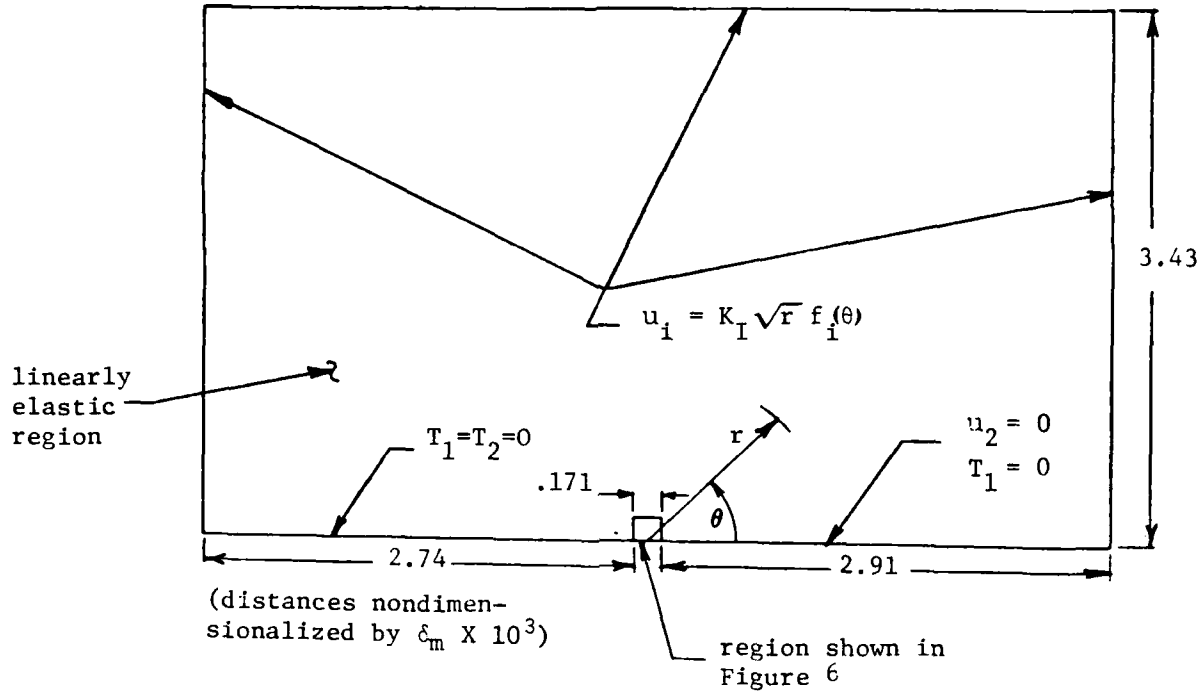

Figure 3. Small scale yielding problem

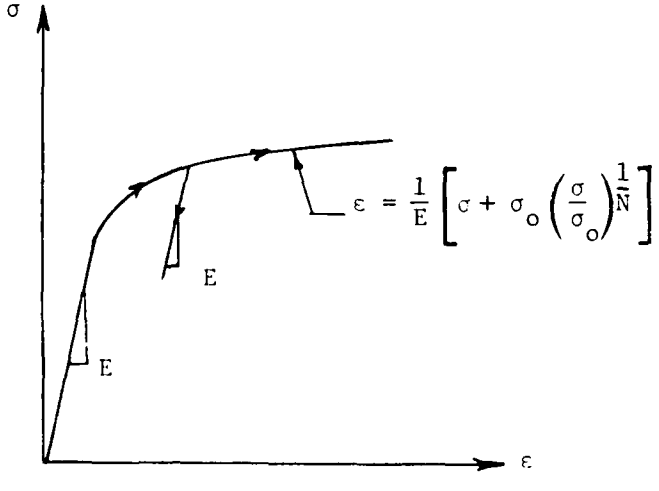

Figure 4. Uniaxial stress-strain diagram

Values used: $E/\sigma_o = 385$
$\nu = 0.3$
$N = 0.077$

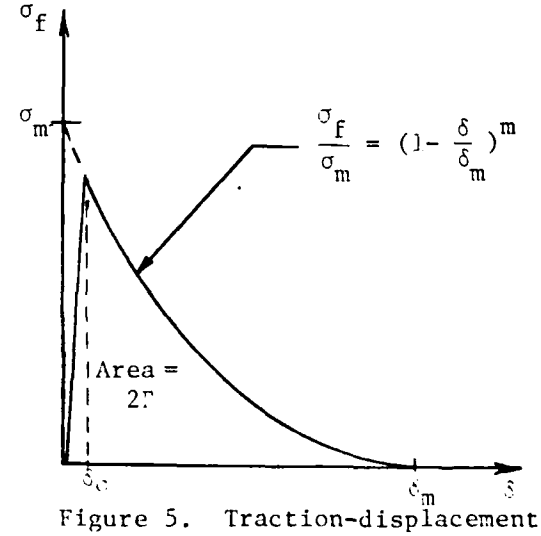

Figure 5. Traction-displacement function for the failure zone

Values used: $\sigma_m/\sigma_o = 2.88$
$\delta_o/\delta_m = 0.002$
$m = 1.05$

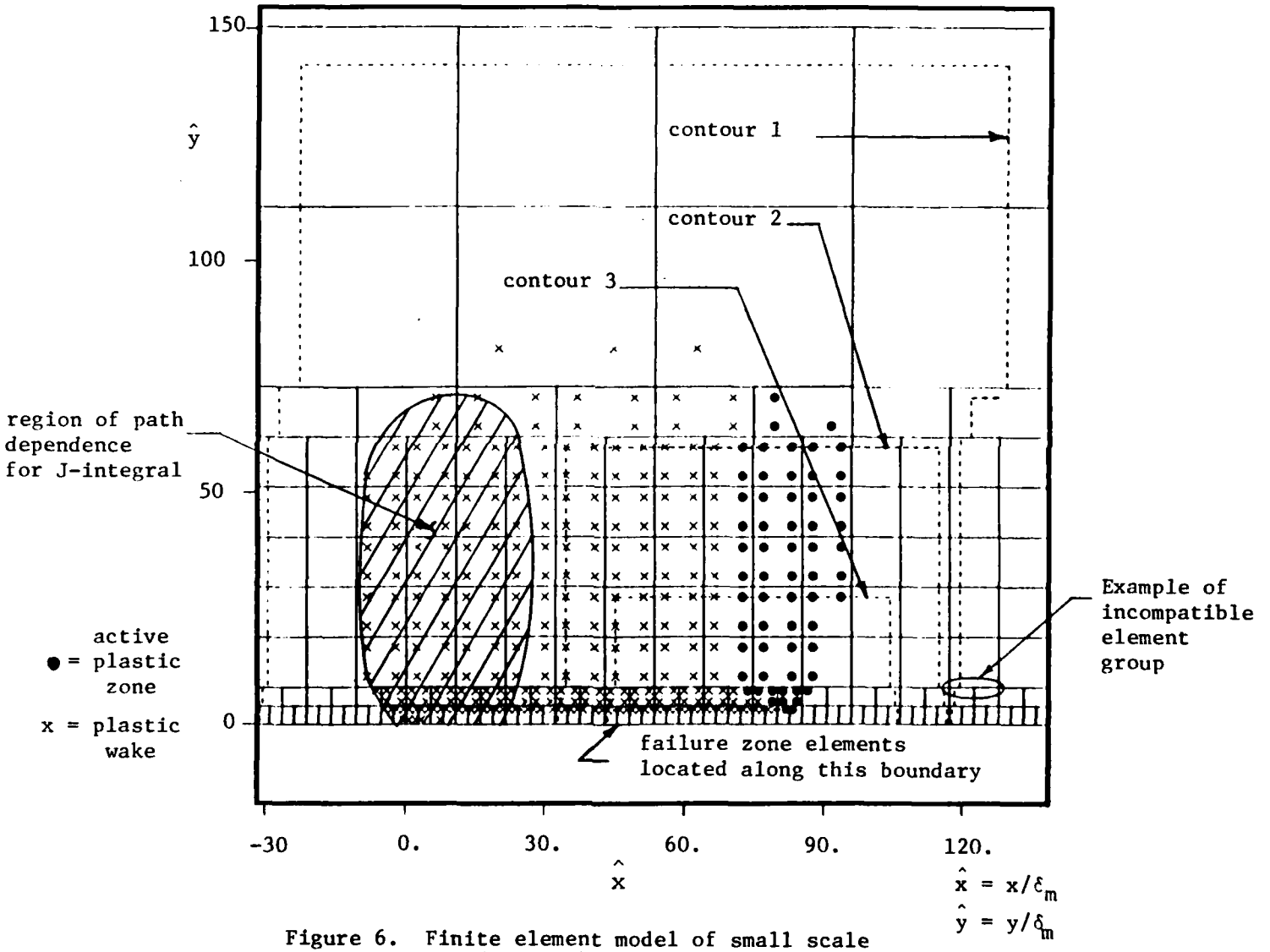

Figure 6. Finite element model of small scale yielding problem after crack advance

of the dimensionless crack advance is shown in Fig. 7. This curve is often called a resistance curve. The energy release rate, $\mathcal{G}$, is defined here by the equation:

$$\mathcal{G} = \frac{1-\nu^2}{E} K_I^2 \tag{8}$$

The crack advance mentioned here is the increase in length, referred to the right end of the failure zone; this end is where the displacement δ_o in Fig. 5 is reached. Results are shown for different meshes, one containing 15 elements in the active plastic zone and the other containing 7 elements in the active plastic zone. It should be noted that while $\mathcal{G}$ increases as the crack advances, the work required to completely separate a ligament of material in the failure zone is constant. The increase in $\mathcal{G}$ is due to the formation of the plastic wake which tends to reduce deformations ahead of the crack below what would be present if the material were truly nonlinearly elastic.

Figure 8 is a plot of τ_{max}/τ_o as a function of $\hat{x}$ for three values of the $\hat{y}$-coordinate. This plot shows a region near the initial crack tip ($\hat{x}$=0) where τ_{max} is above yield and also is a function of the $\hat{x}$-coordinate. Since this violates the requirements for path independence of J, this region must lie outside of the contour path in order to get J values that are path independent and equal to 2Γ. The area of path dependence is shaded in Fig. 6.

When the J-integral is evaluated on a contour that surrounds the crack tip and lies in the linearly elastic region, the relationship [4]

$$J = \frac{1-\nu^2}{E} K_I^2 \tag{9}$$

should hold before and during crack growth. This relationship is found to

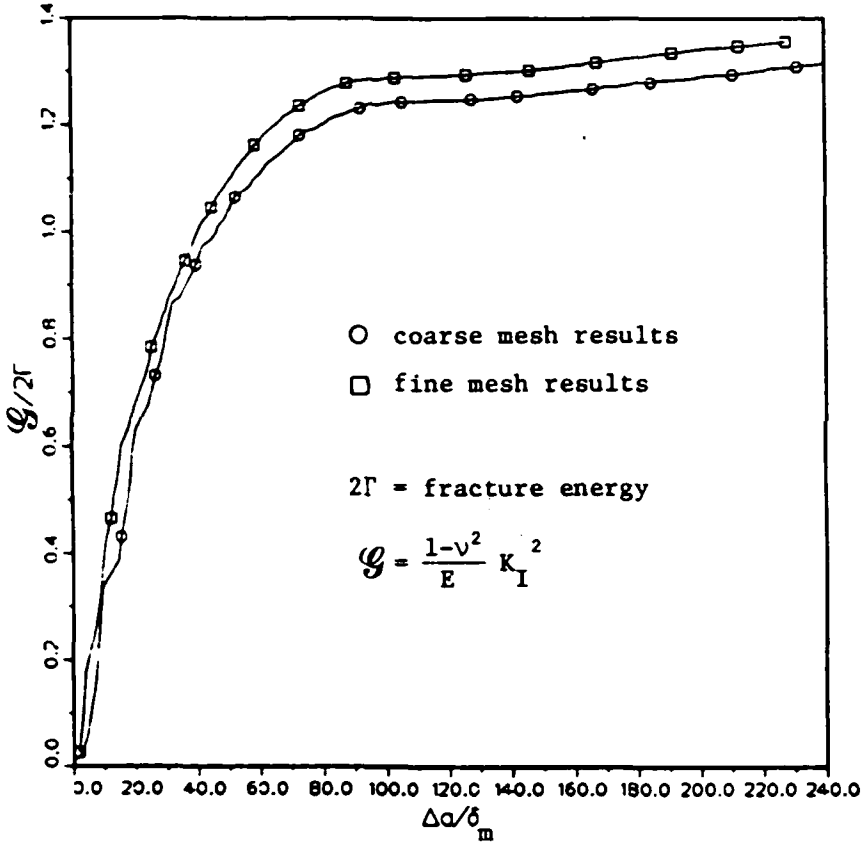

Figure 7. Resistance curve calculated from the finite element model.

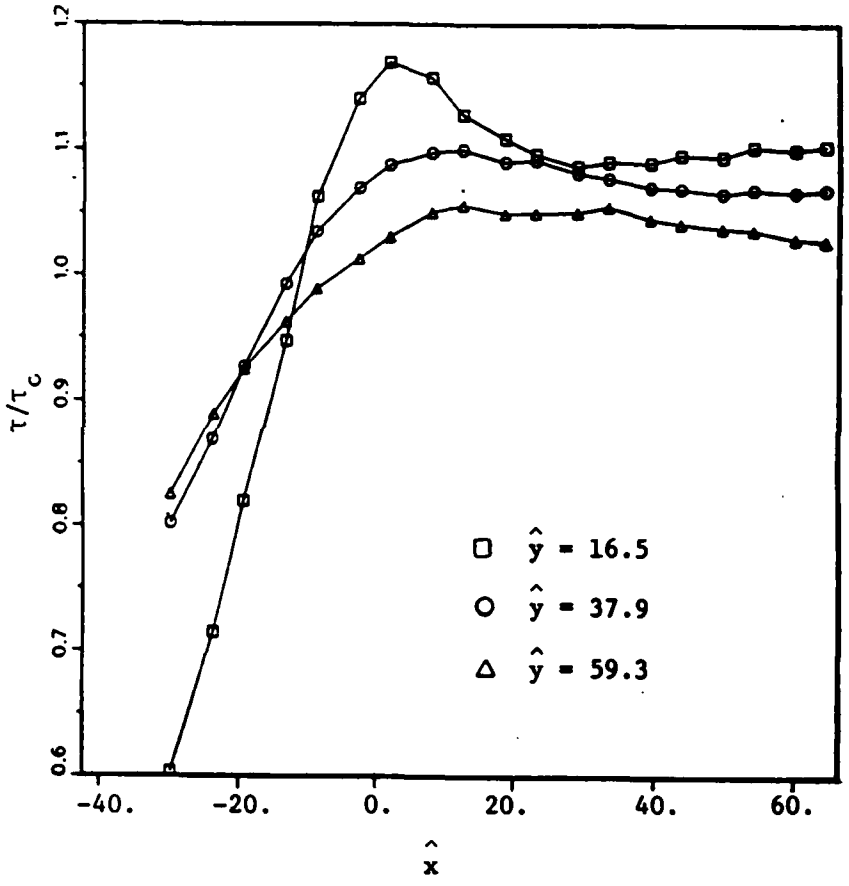

Figure 8. Maximum octahedral shear stress in plastic wake as a function of the horizontal coordinate.

be essentially satisfied for contour 1 in Fig. 6 which surrounds the plastic zone and wake (cf. Table 1). The values of J coming from contours 2 and 3 listed in Table 1 are not equal to $\mathcal{G}$; however, they both have approximately the same value and are equal to the area under the traction-displacement curve given for the failure zone. As expected from theory, contour 4 also gives approximately the same value for J as contours 2 and 3. Figure 9 shows the relationship between contour 4 and contour 1. These results confirm the path independence of J as discussed in [3].

Future work: We plan to study how parameters related to the failure zone (eg. σ_m, δ_m, and m in Fig. 5) affect the resistance curve (Fig. 7) for small scale yielding. Also to be studied is a split beam problem with plastic deformation in which the plastic zone is large compared to the beam height. When generalized to an orthotropic media with damage, the results for the split beam should help us to interpret data from delamination tests on composite materials.

Table 1. J-Integral Calculations

Contour	$J/2\Gamma$
1	1.30
2	.991
3	.994
4	1.04

Eq. (9): $J = \frac{1-\nu^2}{E} K_I^2 = 1.32 \times 2\Gamma$

Contour 1: $J = 1.30 \times 2\Gamma$

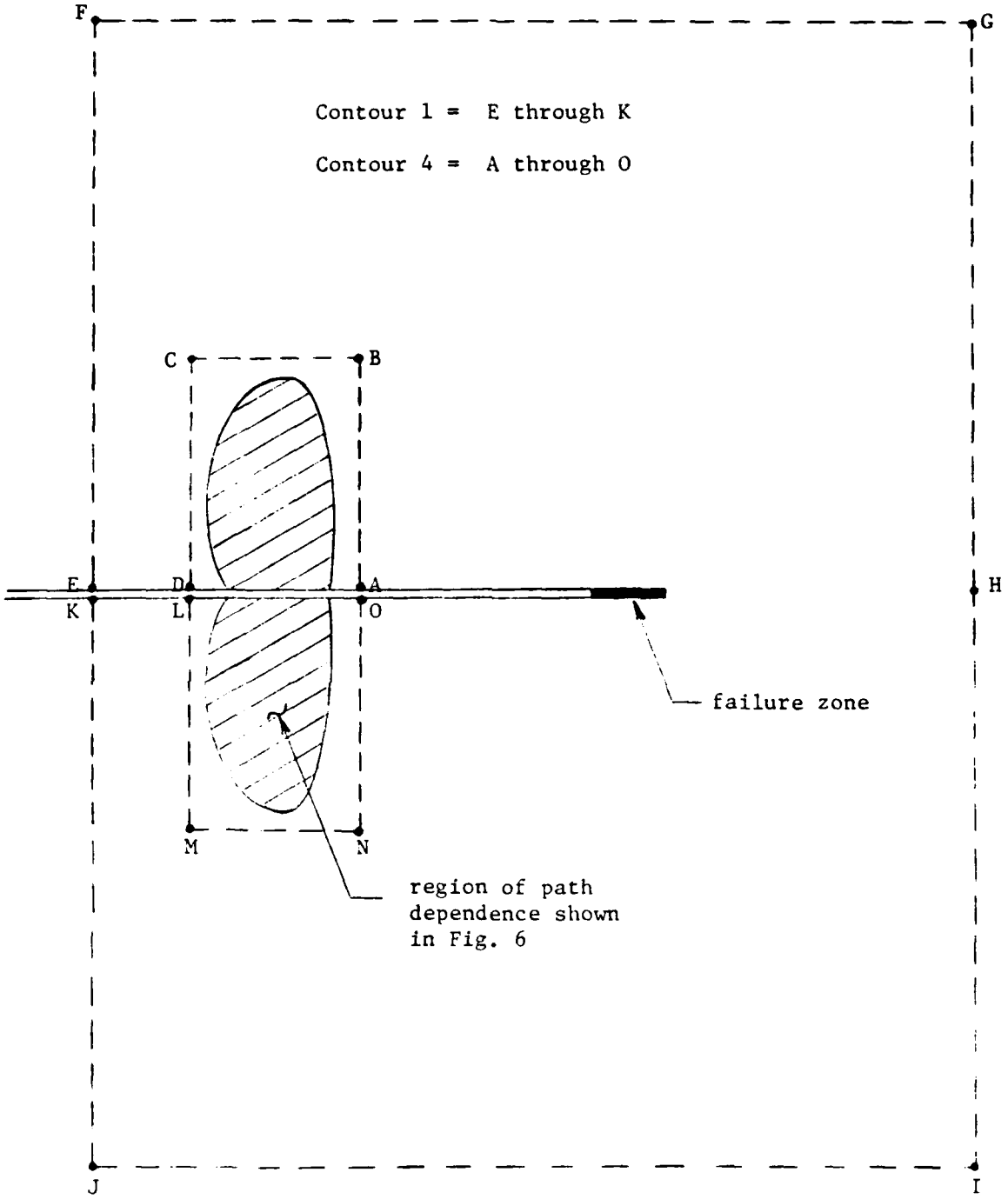

Figure 9. Distinction between contours 1 and 4

2.3 Studies of Unidirectional Bar and Angle-Ply Tube Specimens

The initial, preliminary phase involved testing of standard uniaxial, 30° off-axis, tensile coupons of Hercules AS4/3502 material in a dry, room-temperature state under load histories which included periods of constant rate loading and unloading as well as constant load, as illustrated on page 5 of publication No. 3 in the Appendix. The load history was designed to (i) obtain the type of information needed to determine mathematical representation of the "strain-energy-like" potentials for loading and unloading up to the stresses causing laminate fracture, and (ii) determine the extent of any viscoelastic behavior which may exist with constant and changing damage, and also characterize it mathematically if it is found to be significant.

These preliminary tests indicated that the viscoelastic effects (apart from damage growth) are measurable. The relative magnitude of these effects were not influenced by ply-thickness variations from 6 to 12 plys, nor by the off-axis angle of the specimen, varying from 10° to 90°. The periods of constant load in the test histories used allowed for determination of the significance of the viscoelastic effects in examining the differences between loading and unloading stress-strain curves. The following observations were consistent across the sample spectrum involving different thickness and fiber angles, $\theta \geq 10°$.

(i) At 50% of ultimate levels, between 50% and 80% of the observed deviation between loading and unloading stress-strain curves was attributable to normal viscoelastic effects. The percentage of viscoelastic effects tended to increase as the off-axis angle increased.

(ii) At 75% of ultimate stress level, between 30% and 50% of the observed deviation between loading and unloading stress-strain curves was attributable to the viscoelastic effects, and again this effect tended to increase as the off-axis angle increased.

The amount of viscoelastic behavior relative to damage effects made it necessary to develop a rather elaborate computer-based data reduction and analysis scheme to quantitatively characterize the deformation response. This scheme uses so-called "pseudo-variables" (in this case, axial pseudo-strain ε^R) which is computed using a convolution integral of the form [3],

$$\varepsilon^R = E_R^{-1} \int_0^t E(t-t') \frac{d\varepsilon}{dt'} dt' \qquad (10)$$

where E(t) is the uniaxial relaxation modulus and E_R is a constant, arbitrarily selected reference modulus. With this approach, the material was then characterized precisely like an elastic material with damage, by examining the relationship between stress (σ) and pseudo-strain (ε^R). The technique is believed to essentially "filter out" the viscoelasticity at fixed damage levels. The necessary software has been developed and was used during this period to begin analysis of the data from off-axis specimens using fiber angles of 10, 15, 30, 45, 60, and 90 degrees.

Around November of 1984, we began consideration of the second phase of data collection. It was considered necessary to conduct an experimental and analytical study of angle-ply laminates under multiaxial loading in order to verify the existence and use of a work potential ϕ for modelling realistically large amounts of distributed damage. This type of laminate undergoes significantly more damage prior to global fracture than unidirectional samples, and therefore provides data that enable a more critical evaluation of the work potential theory. The unidirectional ply

studies provide baseline elastic and viscoelastic property data in the absence of the significant residual stresses which exist in angle-ply laminates, and thus can be used to predict baseline angle-ply response with no significant damage. Hercules, Inc. of Magna, Utah, has provided four (4) tube specimens of angle-ply laminates. These were to be tested under axial load and torsion using the MTS hydraulic axial-torsion machine at Texas A&M. If Eq. (12) in [6] was found to be true using data from the tubes, then a potential was to be constructed and expressed as a function of laminate thickness-averaged strains and the extent of damage using suitably defined damage parameters [3]. Physical inspection for damage using x-rays and ultrasound were to be carried out when possible, in order to correlate physical damage stress with characteristics of the stress-strain behavior.

The first set of tubes to be studied consists of two $[\pm 30]_{2S}$ and two $[\pm 60]_{2S}$ tubes, all 2 inch dia x 17 inch long. They were to be tested and the findings analyzed. As the initial task in this study, it was decided to acquire and validate a finite-element routine which would allow for careful and optimized usage of the four tubes available, since the very high cost and long lead times typically required to obtain additional tubes made the tubes quite valuable structures. Analysis of the uniaxial data proceeded, but was secondary to preparing for tube testing which was to begin in January of 1985.

On the morning of December 31, 1984, during an ice storm, the building at the Texas A&M University Research and Extension Center (which housed our HP 1000 computer being used to analyze all the data and to run the finite-element model previously mentioned) burned to the ground in less than one hour. For all practical purposes, all of the data, computer code,

intermediate results and back ups (which were stored in another room of the same building) were reduced to ashes and were totally irretrievable. Needless to say, this tragedy dealt a severe blow to project progress. The code developer was unique to the particular advantages of the HP 1000 vector processing system as was the finite-element code. Subsequent to the fire, attempts have been made to regroup, and some tube testing of isotropic (aluminum) tubes was carried out to verify the test configurations, data acquisition and data analysis techniques. Tube testing could then proceed if a suitable simulation and finite-element code could be developed. Since, however, it would take considerable time to transfer all the code and existing data and techniques to another machine and since Texas A&M University intends to relace the HP 1000 no later than September of 1985, the proposed plan is to place this portion of the project on hold until the new processor is available.

2.4 Studies of Angle-Ply Bars under Axial and Torsional Loading

Preliminary studies of narrow rectangular plates under axial and torsional loading have indicated that they may be very useful for investigations of work potentials with microcracking and delamination fracture behavior. Specimens with different fiber angles and dimensions are under study. Figures 10 and 11 give some data from plates with nominal dimensions of 2.5" long x 0.25" wide x 0.13" thick; the "nominal" stresses and strains shown on the axes are defined below. Plates which are wider and longer and have other fiber angles are also under study. It should be emphasized that even though there are stress gradients and consequent nonuniform damage distributions, the proposed theory based on work potentials may be experimentally verified and then employed to obtain basic fracture properties from such tests without having to make a detailed stress analysis of the specimens. However, some stress analysis will be done to aid the determination of deformation properties, optimize specimen dimensions and select fiber angles.

An important part of the initial study is to demonstrate experimentally that work potentials exist. A theoretical basis for such potentials is given in [6]; but it is based on certain idealizations, and therefore it is important to provide also a good experimental basis for the existence of potentials. Considering here only the problem of elastic laminates with damage under increasing axial force F and torque T, a necessary and sufficient condition for a work potential $\Phi = \Phi(u,\theta)$ to exist (where u is the axial displacement and θ is the rotation about the axis between the grips) is

$$\frac{\partial F}{\partial \theta} = \frac{\partial T}{\partial u} \tag{11}$$

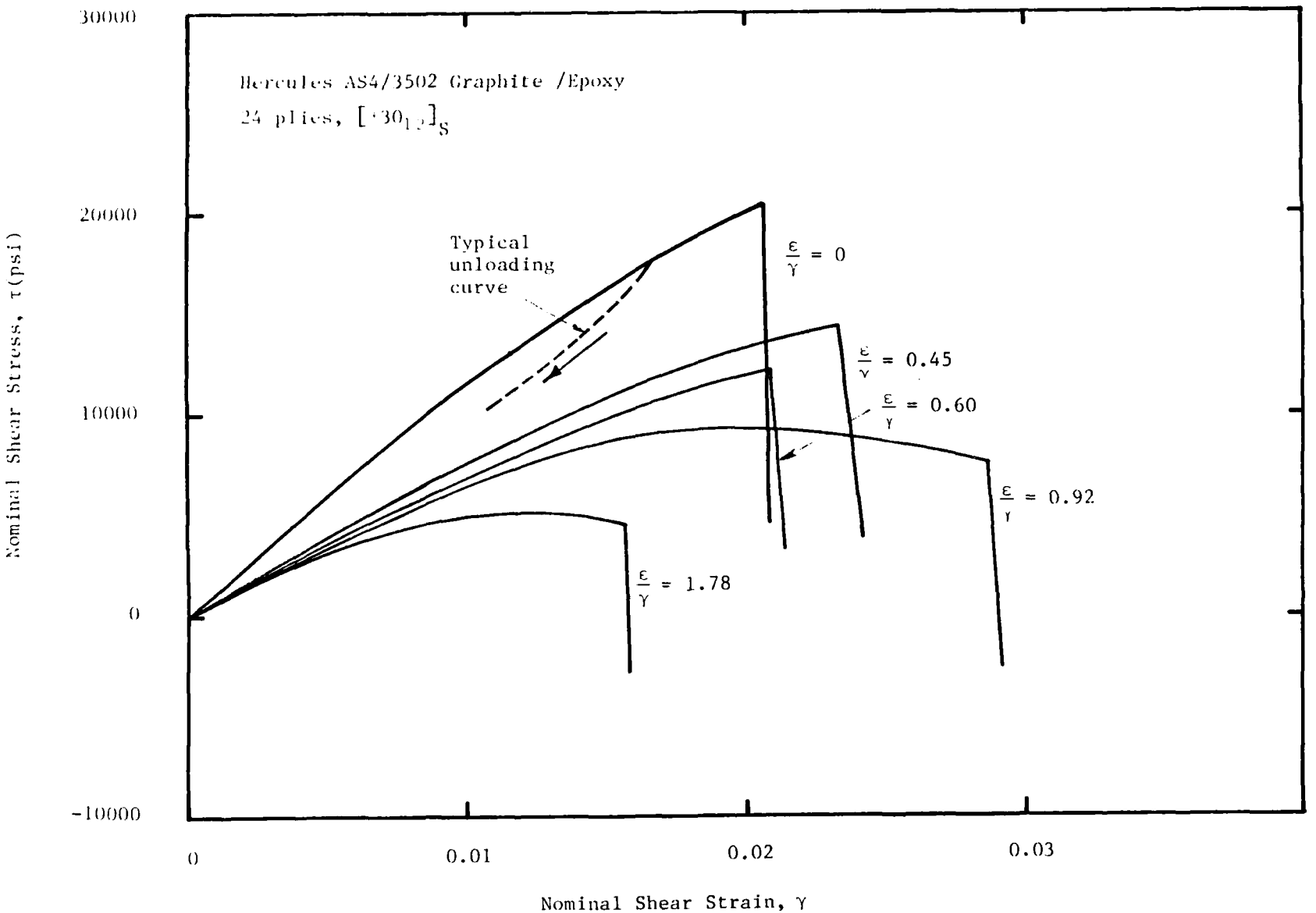

Figure 10. Representative shear stress-strain curves with proportional axial and torsional straining

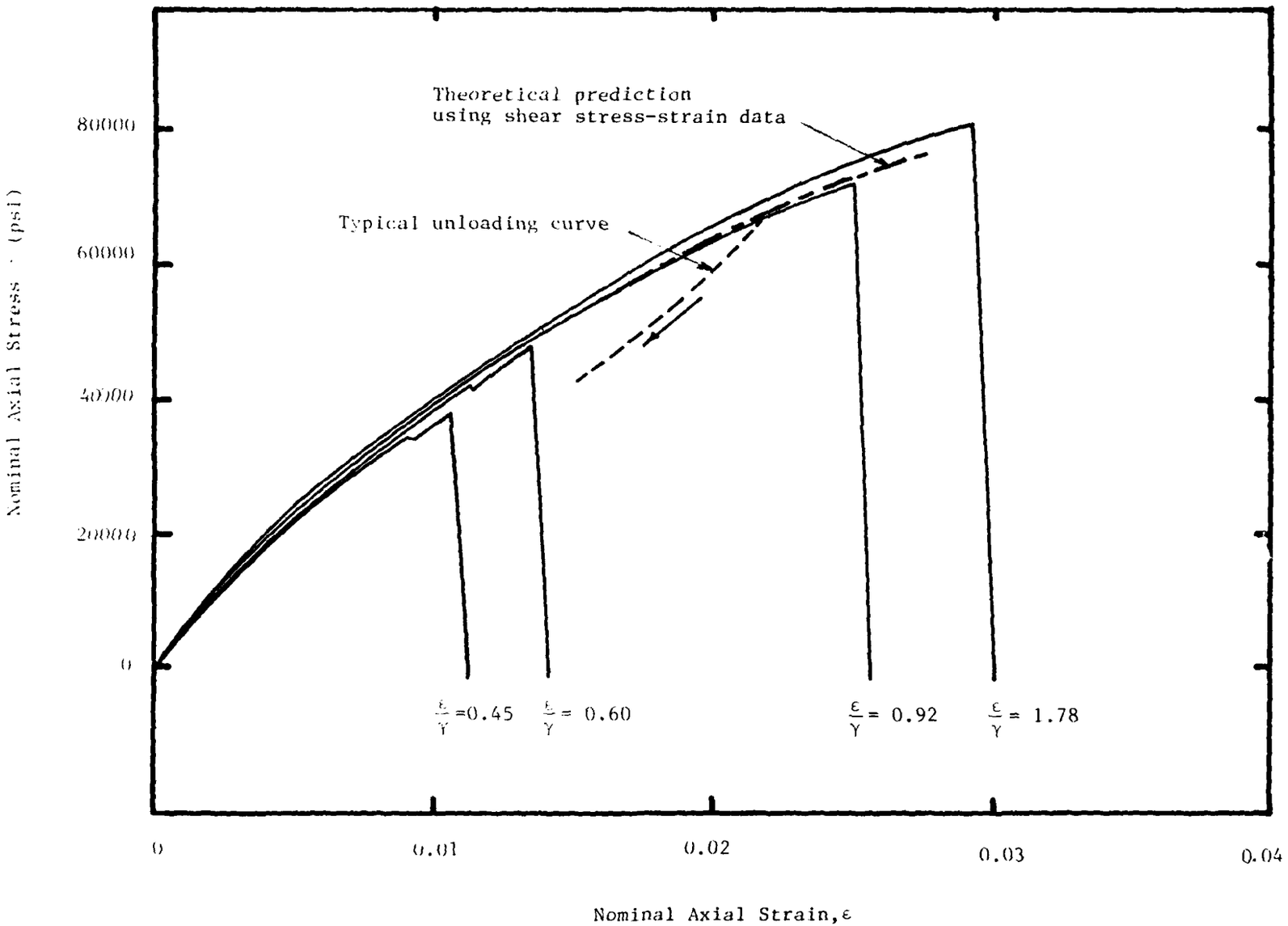

Figure 11. Representative axial stress-strain curves with proportional axial and torsional straining

if $F = F(u,\theta)$ and $T = T(u,\theta)$ have continuous first partial derivatives in their arguments [7, p. 170]. It is assumed there are at least limited sets of histories, $u(t)$ and $\theta(t)$, (such as proportional deformations wherein u/θ is independent of time) for which F and T are essentially independent of history.

Before using Eq. (11) with experimental data, it is helpful to replace the variables by measures of stress and strain. This normalization process eliminates first-order effects of specimen-to-specimen dimension variations. Specifically, we use "nominal" stresses and strains defined as

$$\sigma \equiv F/bc \quad , \quad \tau \equiv 3T/bc^2 \tag{12a}$$

$$\varepsilon \equiv u/L \quad , \quad \gamma \equiv c\theta/L \tag{12b}$$

where b = width, c = thickness, and L = length (between grips). For the special case of long, thin, homogeneous specimens ($L>>b>>c$) σ and ε are the axial stress and strain respectively, and τ and γ are the in-plane shear stress and strain respectively at the surface; this is shown in [8] for linear isotropic materials, and it can be shown to apply also to orthotropic materials whose material axes are parallel to the specimen edges. The variables in Eq. (12) are useful for normalizing data, whether or not the stated conditions apply. Equation (11) becomes

$$\partial\sigma/\partial\gamma = \partial(\tau/3)/\partial\varepsilon \tag{13}$$

This equation has been used to analyze the data in Figs. 10 and 11 by first writing

$$\tau/3 = \tau_o/3 + f \tag{14}$$

where $\tau_o = \tau_o(\gamma)$ is the shear stress for $\varepsilon=0$; also $f=f(\varepsilon,\gamma)$ in which $f(o,\gamma)=0$. Next, integration of Eq. (13) with respect to γ yields

$$\sigma = \frac{\partial}{\partial \varepsilon} \int_0^{\gamma} f(\varepsilon,\gamma')d\gamma' + \sigma_o \tag{15}$$

where $\sigma_o = \sigma_o(\varepsilon)$ is the axial stress when $\gamma=0$. Thus, the quantity

$$\Delta\sigma \equiv \frac{\partial}{\partial \varepsilon} \int_0^{\gamma} f(\varepsilon,\gamma')d\gamma' \tag{16}$$

is the change in axial stress due to the torque-induced shear strain.

The procedure used to check for the existence of a work potential is to cross-plot the data in Fig. 10 so as to obtain f (which is the change in shear stress due to axial strain) as a function of γ, for fixed values of ε, and then predict the modification to axial stress, Eq. (16). Considering the limited amount of data presently available, it is desirable to curve fit the data to analytical expressions to aid the needed interpolations and extrapolations. It was found that

$$\int_0^{\gamma} f(\varepsilon,\gamma')d\gamma' = A\gamma^{2.55}\varepsilon^{(B+C\gamma)} \tag{17}$$

where A,B, and C are constants. Using this expression in Eq. (16) yields the change in axial stress due to torsion. Only for $\varepsilon/\gamma = 0.92$ is there a significant effect of torsion prior to fracture; the prediction is drawn in Fig. 11. The agreement between theory and experiment is relatively good.

In the series of tests shown in Figs. 10 and 11 there is only one specimen for each deformation history, and thus the small differences between most curves in Fig. 11 could be as large as specimen-to-specimen differences. Nevetheless, it is encouraging that all of the predictions from Eq. (16) turn out to be of the same order as the observed differences in normal stress. Although not needed to check for the existence of a potential, it is of interest to note that when there is little or no

coupling between torque and axial load, the stress-strain curves obey power laws over a wide range of strains, as shown in Fig. 12.

Future Work: It is planned to continue the axial-torsion testing of angle-ply bar specimens to study both deformation history effects and determine the range of histories for which work potentials exist. Mode III delamination will be investigated also using specimens with and without embedded edge delaminations. In most tests conducted so far, fracture occurs away from the grips, and therefore it is believed this study will lead to basic results on the effect of globally distributed microcracks in a multiaxial stress state on macrocrack growth (e.g., the edge delamination). The J integral will be used with the data to characterize the mode III fracture initiation and propagation behavior.

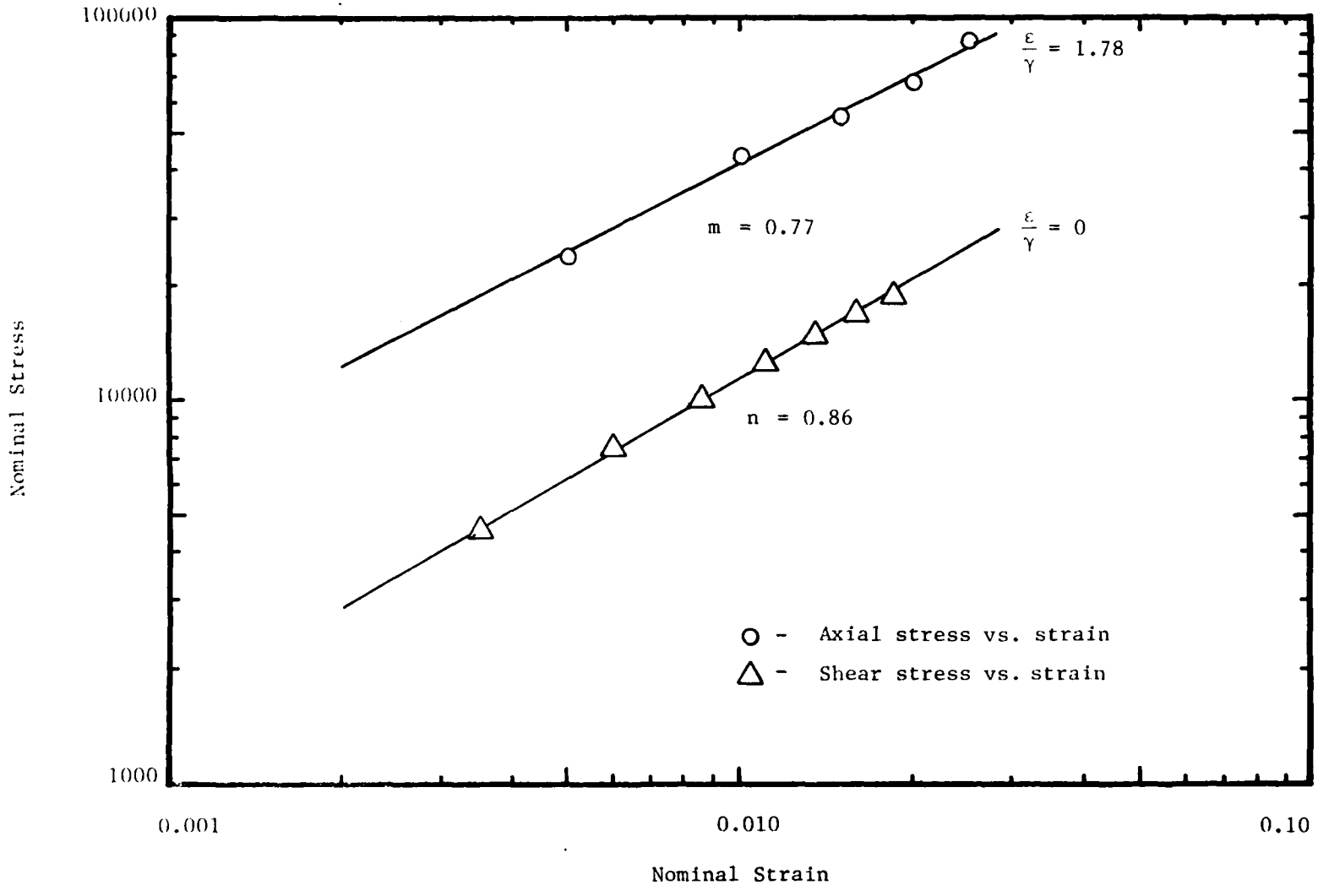

Figure 12. Logarithmic plots of stress-strain data from Figures 10 and 11 showing power law behavior

3. LIST OF AFOSR SPONSORED PUBLICATIONS

3.1 Published during project year:

Schapery, R.A., "Correspondence Principles and a Generalized J Integral for Large Deformation and Fracture Analysis of Viscoelastic Media," Int. J. Fracture, 25 (1984) pp. 195-223.

3.2 To be published (in press);

Schapery, R.A., "Continuum Aspects of Crack Growth in Time-Dependent Materials", Encyclopedia of Materials Science and Engineering, Pergamon Press.

Schapery, R.A., "Deformation and Fracture Characterization of Inelastic Nonlinear Materials Using Potentials," Polymer Preprints.

3.3 To be submitted for publication:

Allen, D.H., Groves, S.E., Harris, C.E. (Part II), and Schapery, R.A., "A Damage Model for Continuous Fiber Composites", Parts I and II (essentially complete) - to be submitted to Mechanics of Materials.

4. PROFESSIONAL PERSONNEL INFORMATION

4.1 List of Professional Personnel

1. Richard Schapery, Principal Investigator
2. Mark Lamborn, Graduate Research Assistant
3. Richard Tonda, Graduate Research Assistant
4. Randy Weatherby, Graduate Research Assistant
5. Bob Harbert, Assistant Research Engineer, (Laboratory Staff Member)
6. Carl Fredericksen, Electronics Technician, (Laboratory Staff Member)

4.2 Spoken Papers (Principal Investigator's Activities)

1. "A J Integral for Viscoelastic Fracture Analysis," ASME/AMD Conference, San Antonio, June 1984.
2. "Research Directions for the Mechanics of Composites,"ASME/AMD Conference, San Antonio, June 1984.
3. "Deformation Properties of Composites", Progress in Paper Physics: A Seminar, Stockholm, June 1984. Also chairman of workshop on deformation properties.
4. "Behavior of Composites with Distributed Damage", Owens-Corning Fiberglas Corp., Granville OH, Oct. 1984.
5. "Matrix Controlled Deformation and Fracture Analysis of Fibrous Composites" Tenth Annual Mechanics of Composites Review, Dayton OH, Oct. 1984.
6. "Mechanics of Deformation and Fracture of Polymeric Materials", (three lectures), National Taiwan Univ., Taipei, Jan. 1985.

5. REFERENCES

[1] Hillerborg, A. and Peterson, P.E., "Fracture Mechanical Calculations, Test Methods, and Results for Concrete and Similar Materials", Advances in Fracture Research (Fracture 81), Vol. 4, Pergamon Press, 1982, pp. 1515-1522.

[2] Aronsson, C., "Tensile Fracture of Composite Laminates with Holes and Cracks", PhD. dissertation, The Royal Institute of Technology, Stockholm, Sweden, 1984.

*[3] Schapery, R.A., "Correspondence Principles and a Generalized J-Integral for Large Deformation and Fracture Analysis of Viscoelastic Media", International Journal of Fracture, Vol. 25, 1984, pp. 195-223.

[4] Rice, J.R., "A Path Independent Integral and the Approximate Analysis of Strain Concentration by Notches and Cracks," J. Applied Mechanics, Vol. 35, 1968, pp. 379-386.

[5] Crisfield, M.A., "A Fast Incremental/Iterative Solution Procedure that Handles 'Snap-Through'", Computers and Structures, Vol. 13, 1981, p. 55-62.

*[6] Schapery, R.A., "Deformation and Fracture Characterization of Inelastic Nonlinear Materials using Potentials," Polymer Preprints, 1985.

[7] Greenberg, M.D., Foundations of Applied Mathematics, Prentice-Hall, Inc., 1978.

[8] Timoshenko, S.P. and Goodier, J.N., Theory of Elasticity, McGraw-Hill Book Co., 3rd Ed., 1970.

*Paper is in the Appendix.

APPENDIX

Publications on AFOSR project:

1. "Correspondence Principles and a Generalized J Integral for Large Deformation and Fracture Analysis of Viscoelastic Media."
2. "Deformation and Fracture Characterization of Inelastic Nonlinear Materials Using Potentials."
3. "Matrix Controlled Deformation and Fracture Analysis of Fibrous Composites." (Set of viewgraphs used at Tenth Annual Mechanics of Composites Review)

International Journal of Fracture 25 (1984) 195–223

Correspondence principles and a generalized *J* integral for large deformation and fracture analysis of viscoelastic media

R.A. SCHAPERY

Mechanics & Materials Center, Civil Engineering Department, Texas A&M University, College Station, TX 77843, USA

(Received June 3, 1983; in revised form March 7, 1984)

Abstract

Methods of quasi-static deformation and fracture analysis are developed for a class of nonlinear viscoelastic media and sample applications are given. Selection of the class of media is guided by actual rheological behavior of monolithic and composite materials as well as the need for simplicity to be able to understand the effect of primary material and continuum parameters on crack growth behavior. First, pertinent aspects of J integral and energy release rate theory for nonlinear elastic media are discussed. Nonlinear viscoelastic constitutive equations are then given, and correspondence principles which establish a simple relationship between mechanical states of elastic and viscoelastic media are developed. These principles provide the basis for the subsequent extension of J integral theory to crack growth in viscoelastic materials. Emphasis is on predicting mechanical work available at the crack tip for initiation and continuation of growth; some examples show how viscoelastic properties and the J integral affect growth behavior. Included is the problem of a crack in a thin layer having different viscoelastic properties than the surrounding continuum. The Appendix gives an apparently new constitutive theory for elastic and viscoelastic materials with changing microstructure (e.g. distributed damage) and indicates the conditions under which the fracture theory in the body of the paper is applicable.

1. Introduction

Methods for characterizing and predicting crack growth in materials which are elastic (except for the small-scale inelastic zone at crack tips) are well-established theoretically, and considerable experimental confirmation exists [1,2]. The methods for linear media now commonly use criteria for initiation and continuation of crack growth which are expressed in terms of stress intensity factors or energy release rate. For nonlinear media, especially rubber [2], energy release rate is often employed.

Fracture theory for materials exhibiting large scale inelastic behavior is considerably more limited. The J integral theory [1,3] has been successfully applied to initiation of crack growth in time-independent (elastoplastic) isotropic, homogeneous media under small strains. An analogous parameter, the C^* integral [4], has served in a similar manner to define crack speed in nonlinear viscous bodies. Analytical methods and their verification for crack growth in viscoelastic media are mainly limited to linear isotropic, homogeneous materials, although some theoretical results exist for linear orthotropic and nonhomogeneous materials [e.g., 5–9]; stress intensity factor is the primary characterizing parameter for fracture initiation time and crack speed.

The objective of much of the work on elastic and inelastic materials has been to identify a basic crack-growth controlling parameter, such as stress intensity factor or the J integral, which accounts entirely for the geometry of a body (including crack geometry) and the applied loads. Values of the parameter which produce crack initiation and various crack

speeds are then found for a given material, usually experimentally. This information may be used to predict crack growth in different geometries and aid in the selection and design of fracture-resistant materials and structures. It is, of course, very important that the characterizing parameter account fully for the effect of geometry and loading conditions on crack growth if empirical corrections for each application are to be avoided.

In this paper we show that parameters analogous to the J integral and energy release rate may be used for quasi-static crack growth in a class of nonlinear viscoelastic materials under finite strain. In Section 2, results on the J integral and energy release rate for three-dimensional deformation of nonlinear elastic media are collected. Included is a simple (and apparently new) derivation of the relationship between the J integral and energy release rate. The J integral formulation is guided by Chen and Shield's work [10,11], and interpretations are given which are used for subsequent application of the theory to viscoelastic fracture.

Viscoelastic constitutive equations and methods of quasi-static deformation analysis using elastic solutions (correspondence principles) are discussed in Sections 3 and 4, respectively. Correspondence principles are given for a broader class of problems than considered in the fracture analysis; for example, they represent a new approach to analyzing crack closing and healing phenomena and ablation effects.

Sections 3 and 4 provide the basis for using the J integral and energy release rate in nonlinear viscoelasticity problems. This generalization, along with results in Section 5 for mechanical work input to the crack tip, is applied in Section 6 to relate fracture initiation time and crack speed to the J integral and viscoelastic properties of the continuum and failing material at the crack tip; these relationships represent extensions of the author's other work [12] based on a two-dimensional J integral and small strains. Then, as another application of the theory, in Section 6 we also predict the effect on crack speed of the rheological properties of a zone of damaged or otherwise special material *surrounding* the crack tip. In practice, viscoelastic behavior of this zone is often significantly different from that of the far field as a result of high local stresses, dissipative heating, or the particular physical situation; the craze zone near crack tips in glassy polymers [13] and an adhesive interlayer are important examples. Surface or path-independence of the J integral exists for materials with certain types of distributed damage as shown in the Appendix; we use this important property here in accounting for behavior of the material surrounding the crack tip.

The deformation and crack growth theory in this paper is not much more involved than that of nonlinear elasticity or special cases of linear viscoelasticity. This simplicity, compared to what one would expect for nonlinear viscoelasticity, is a direct result of the particular constitutive equations and mechanical variables selected to characterize rheological behavior. We believe the theory provides a practical approach to the development of realistic damage and global fracture models for nonlinear elastic, viscous, and viscoelastic media, as illustrated by the author for a particulate composite material and polycrystalline metal [14,15].

2. The reference elastic problem

Certain basic equations for elastic materials under large strains are summarized in this section. They are expressed in terms of stresses σ_{ij}^R $(i, j = 1, 2, 3)$ and displacements u_i^R referred to an orthogonal set of Cartesian coordinates x_i which define the location of material points in the undeformed state of the body, B_0. (Although B_0 is called the "undeformed state", it could be any fixed reference configuration, such as that existing at one time during the actual deformation history, without necessitating a change in the basic theory.) The instantaneous Cartesian coordinates y_i^R of material points in the deformed

body B^R are referred to the same fixed axes as used for B_0, and therefore $y_i^R = u_i^R + x_i$. In some cases σ_{ij}^R or u_i^R will be equal to the stresses or displacements in a viscoelastic body; but in general they are different, and therefore the superscript R is used to make this distinction. Section 4 is concerned with the correspondence between states of elastic and viscoelastic bodies. For now we shall just list and discuss relevant equations for elastic media.

The stresses σ_{ij}^R are taken to be the components of the so-called *Piola* stress field [16]. The components of the Lagrangian stress tensor T_{ij}^R [17] are given by the transpose of σ_{ij}^R; viz., $T_{ij}^R = \sigma_{ji}^R$. Although σ_{ij}^R is not in general symmetric, these components are very convenient for our purposes because the equilibrium equations,

$$\partial \sigma_{ij}^R / \partial x_j + F_i^R = 0 \tag{1}$$

and the relation between surface tractions T_i^R and stresses,

$$T_i^R = \sigma_{ij}^R n_j \tag{2}$$

are identical in form to those in the linear theory. (Throughout this paper the summation convention is followed wherein repeated indices imply summation over their range unless stated otherwise.) All quantities are referred to B_0, in which x_i are the independent variables. Namely, F_i^R is body force per unit undeformed volume, T_i^R is the surface force per unit undeformed area, and n_j is the outer unit normal of an area element defined in the undeformed state; force quantities are defined as the vectors existing at the current time t, but referred to the undeformed geometry, B_0.

A potential Φ is assumed to exist with the property that

$$\sigma_{ij}^R = \partial \Phi / \partial \left(u_{i,j}^R \right) \tag{3}$$

where, by definition,

$$u_{i,j}^R \equiv \partial u_i^R / \partial x_j. \tag{4}$$

For an elastic material Φ is the strain energy per unit undeformed volume [17]. If we invoke the physical requirement that Φ is unaffected by rigid body rotation (and recall that we are using the coordinates x_i as the independent spacial variables) the dependence of Φ on the displacement derivatives can enter only through the symmetric Green's strain tensor [26],

$$E_{ij}^R = (1/2)\left[u_{i,j}^R + u_{j,i}^R + u_{k,i}^R u_{k,j}^R \right] \tag{5}$$

However, considering the association between the present elastic problem and the actual (viscoelastic) problem introduced later, we shall not restrict Φ by this usual physical condition. Instead, unless stated otherwise, we suppose only that

$$\Phi = \Phi\left(u_{i,j}^R, x_2, x_3, t \right) \tag{6}$$

implying possible dependence on the nine displacement derivatives, spacial variables x_2, x_3 (allowing for nonhomogeneity with respect to x_2 and x_3) and time t (allowing for "aging" changes). The body is assumed to be homogeneous with respect to x_1 for now to achieve surface-independence of an integral that is useful in fracture analysis. With the same objective in mind, we assume a body force potential $\Phi_f = \Phi_f(u_i^R, x_2, x_3, t)$ exists, in which

$$F_i^R = -\partial \Phi_f / \partial u_i^R \tag{7}$$

Consider a generic volume V throughout which Φ and Φ_f exist with properties defined by Eqns. (3) and (7). Denote the bounding surface of this generic volume by S and let T_i^R

be the surface tractions and n_j the components of the outer unit normal. Multiply (1) by $-\partial u_i^R/\partial x_1$, integrate over the volume V, and then use the divergence theorem [18] to convert the integral to an integral over the surface S. The result is

$$\mathcal{J} \equiv \int_S \left[(\Phi + \Phi_F)n_1 - T_i^R \partial u_i^R/\partial x_1\right] ds = 0 \tag{8}$$

where ds is an area element in the undeformed body. When $\Phi_F = 0$ and the body is homogeneous, the integral $\mathcal{J}$ becomes identical to the x_1 component of the integral vector derived by Knowles and Sternberg [16]; however, we have followed Chen and Shield [10] and not limited Φ to dependence on strains. By considering only the x_1 component, material nonhomogeneity with respect to x_2 and x_3 may be taken into account while retaining the property that $\mathcal{J} = 0$. Only this component is needed in the fracture analysis to follow.

The J integral and crack tip model

Suppose the body contains one or more cracks. Figure 1 shows as an idealization the intersection of a crack tip region and local crack faces with the plane of the page. The dashed line is the intersection of a representative surface S with the same plane. In order to meet the conditions which lead to $\mathcal{J} = 0$, no crack can exist inside or on S.

The region designated as the failure zone in Fig. 1 is where material separation occurs; it may contain a high density of microcracks or microvoids. The material comprising this zone in the undeformed state is of length α (not necessarily small) and is assumed to exist in a layer which is thin (in the x_2 direction) relative to α. Outside of the failure zone it is assumed there exists at least a small neighborhood around the crack tip for which $\mathcal{J} = 0$. A useful definition of the crack tip P, and one that we employ, is that it is the leading edge of the material for which the conditions used in deriving $\mathcal{J} = 0$ are *not* met.

It should be noted that tractions may exist along the crack faces to the left of the failure zone; for example, these may be due to a pressurized fluid, interfacial friction and contact pressure, or damaged material connecting the faces of the intact continuum (as in a craze zone in some plastics). In these cases, especially the last one, location of the left end of the failure zone (points 1 and 2) is somewhat arbitrary and its selection may depend on the

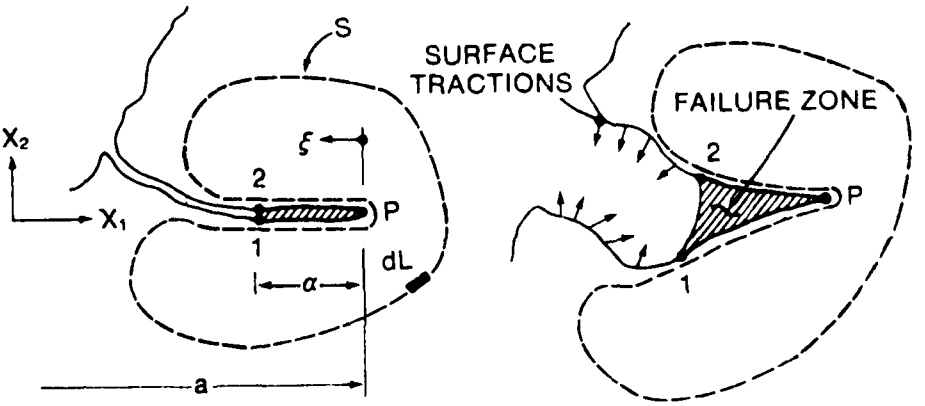

(a) Undeformed body. (b) Deformed body

Figure 1. Cross-section of crack in neighborhood of the tip P. The region of intense damage and material separation processes is designated the failure zone, whose length is α in the undeformed body

particular application of interest. However, normally one would choose it so that α extends at least over the part of the surface $x_2 = 0$ for which crack tip material behavior is too complex to be able to predict the detailed traction distribution.

Next, we introduce the integral J_f:

$$J_f \equiv \int_0^{\alpha} \tau_i^R \frac{\partial \Delta u_i^R}{\partial \xi} d\xi \tag{9}$$

where τ_2^R is the normal stress and τ_1^R and τ_3^R are the shearing stresses in the x_1 and x_3 directions, respectively, along the interface between the failure zone and continuum: these are Piola stresses, as defined previously. It is assumed that the failure zone is sufficiently thin that the stresses in Eqn. (9) are the same along both top and bottom portions of the interface. The Δu_i^R are the components of the relative displacement vector between initially adjacent interface points across the local crack plane $x_2 = 0$. The viscoelastic normal stresses, τ_2 and σ_{22}, and displacement, $\Delta u_2/2$, along the upper surface of the continuum are indicated in Fig. 2. By definition, for the elastic or viscoelastic problem, the "relative displacement vector" is the displacement vector at the failure zone-continuum interface above the local crack plane minus that below this plane.

For later use we shall suppose that the crack tip or edge P is essentially straight and parallel to the x_3 axis over at least a short distance l_3 from the plane of the page ($x_3 = 0$). Over this same distance it is assumed the failure zone integral J_f does not vary. Since $n_1 = 0$ along the top and bottom interfaces it is readily shown that the contribution to $\mathcal{A}$, (8), from the portion of S along the top and bottom boundaries of the failure zone over the crack edge of length l_3 is equal to $-J_f l_3$, assuming the integral over the small curved surface at the tip P can be neglected; this latter assumption is reasonable as long as the undeformed failure zone layer is thin relative to α and we impose the physical requirement of finite stresses (including those at P). Thus, from the condition $\mathcal{A} = 0$,

$$J_\infty = J_f \tag{10}$$

where

$$J_\infty \equiv (1/l_3) \int_{S_1} \left[(\Phi + \Phi_f) n_1 - T_i^R \frac{\partial u_i^R}{\partial x_1} \right] ds \tag{11}$$

and S_1 is the portion of S not included in the integration along the failure zone over the length l_3.

Notice that J_∞ is a surface-independent integral in that its value is the same (i.e. J_f)

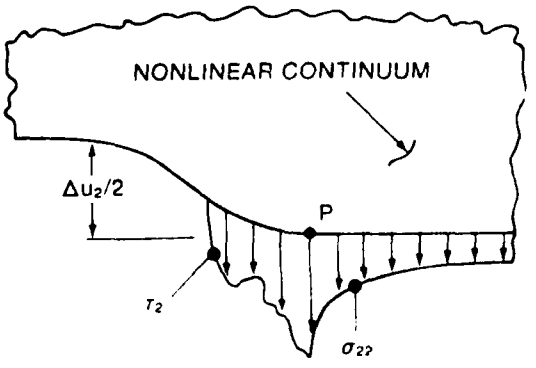

Figure 2. Normal stresses and opening displacement along continuum above local crack plane.

regardless of the choice of S_1 except for the conditions stated above. It can be reduced to Rice's path-independent J integral [3] by omitting the body force and assuming two-dimensional deformations. Specifically, let S be a cylinder (having the cross-section in Fig. 1) with generators and with normals to the end areas which are parallel to x_3. At the ends $n_1 = 0$, and therefore the contribution to J_v from the cylinder ends vanishes if $T_i^R \partial u_i^R/\partial x_1 = 0$; this condition exists on the ends when $T_i^R = 0$ (e.g. plane stress) or $T_1^R = T_2^R = \partial u_3^R/\partial x_1 = 0$ (e.g. plane strain) or $T_3^R = \partial u_1^R/\partial x_1 = \partial u_2^R/\partial x_1 = 0$ (e.g. antiplane strain). With the integrand in (11) further assumed to be independent of x_3,

$$J_v = \int_{C_1} \left[(\Phi + \Phi_F) \mathrm{d}x_2 - T_i^R \frac{\partial u_i^R}{\partial x_1} \mathrm{d}L \right] \tag{12}$$

where the integration path C_1 starts at point 1 in Fig. 1 and proceeds counterclockwise to point 2. Assuming $\Phi_F = 0$, crack faces parallel to x_1 and traction-free, small strains and rotations, and further that Φ is a function of $u_{i,j}^R$ through the strains, (12) reduces to the original form of Rice's J integral.

Suppose S_1 in the three-dimensional version of J_v, (11), is chosen so as to not include any portion of the failure zone-continuum interface (outside of l_3). We may then consider (10) to give a basic relationship between the mechanical state of the continuum through J_v and the characteristics of the failing material along a segment of the crack edge. In some cases one may want to use a failure zone integral in which l_3 includes the entire crack edge (or a large segment of it). If the integral (9) is not constant or the edge is not straight along the length of interest, one would return to (8) to derive the desired form, accounting as necessary for curvature of the edge.

Finally, it should be noted that (10) and (11) *do not* depend on crack faces being parallel to the $x_1 - x_3$ plane. Rather, this condition is imposed only on the layer of material comprising the undeformed failure zone.

Energy release rate

Up to now we have not considered crack growth. By introducing a virtual crack extension, the value of J_v can be related to a global change in energy. This relationship may be useful for the experimental or theoretical determination of J_v for elastic and viscoelastic materials, as an alternative to evaluating it directly from the integral, (11). The desired equation may be derived by first multiplying (1) by a change in displacement δu_i^R, integrating over the volume V of B_0, and using (2), (3), (4), and (7) along with the divergence theorem. There results, finally, the familiar equation for virtual work,

$$\int_S T_i^R \delta u_i^R \mathrm{d}s = \delta \int_V (\Phi + \Phi_F) \mathrm{d}v \tag{13}$$

Both S and V have been assumed constant in deriving this result; e.g., there is no explicit change in crack tip location or phenomena such as material removal through melting. Crack growth will be simulated through a suitable choice of δu_i, as in [14], thus permitting the use of (13). An edge segment of length l_3 (in the x_3 direction) of only one of possibly many cracks in the body is to be advanced an amount δa, as illustrated in Fig. 3; this advancement is assumed independent of x_3. The interface between the failure zone material and continuum of undeformed planar dimensions $(a + \delta a)$ by l_3 is denoted as S_f and considered to be a portion of S in (13). As before, we denote by Δu_i^R the current relative displacement components between originally adjacent material points across the local crack plane (which are specifically the displacements between the portions of S_f above and below the crack plane). Self-similar crack growth is now imposed: $\Delta u_i^R = \Delta u^R(\xi)$

Recall that (10) is dependent on the assumption that the material is physically homogeneous in the x_1 direction for the portion of the continuum bounded by the failure zone and the surface S_1 used in (11). In contrast, this assumption is *not* needed to derive (17), in that Φ, Φ_F, and Φ_T in (18) may depend explicitly on all coordinates x_i (as well as on displacement derivatives or displacements, as previously indicated).

Finally, it is to be observed that when surface tractions on S_T or body forces are specified functions of x_i, *or treated as such*, the potentials are

$$\Phi_F = -F_i^R u_i^R, \quad \Phi_T = -T_i^R u_i^R. \tag{21}$$

Equation (18) then takes the familiar form,

$$P_e = \int_V (\Phi - F_i^R u_i^R)\mathrm{d}v - \int_{S_T} T_i^R u_i^R \mathrm{d}s. \tag{22}$$

For elastic materials, the quantity P_e is the potential energy. Its physical significance is somewhat different for the class of viscoelastic materials discussed in the next section.

3. Viscoelastic constitutive equations

The constitutive equations which will be used are based on (3), but the displacements u_i^R and stresses σ_{ij}^R are not necessarily physical quantities in the viscoelastic body. Instead, they are related to the physical displacements $u_i(x_k, t)$ and stresses $\sigma_{ij}(x_k, t)$ through hereditary integrals.

Specifically, considering displacements first, and assuming they vanish for $t < 0$,

$$u_i^R = E_R^{-1} \int_0^t E(t-\tau, t) \frac{\partial u_i}{\partial \tau} \mathrm{d}\tau \tag{23}$$

where $u_i = u_i(x_j, \tau)$ is the physical displacement in terms of the time variable of integration, τ, and, as before, the coordinates x_j of the undeformed body. The quantity $E = E(t-\tau, t)$ is called a *relaxation modulus*, which imparts hereditary characteristics to the deformation behavior. The coefficient E_R is a free constant which will be termed the *reference modulus*; it is helpful in discussing special material behavior and introducing dimensionless variables. In order to allow for the possibility of a discontinuous change in u_i with time at $t = 0$, the lower integration limit in (23) and succeeding hereditary integrals should be interpreted as 0^- unless indicated otherwise. The inverse of (23) is

$$u_i = E_R \int_0^t D(t-\tau, t) \frac{\partial u_i^R}{\partial \tau} \mathrm{d}\tau \tag{24}$$

where $D = D(t-\tau, t)$ is termed a *creep compliance*. It is readily shown that E and D satisfy

$$\int_{t_0}^t D(t-\tau, t) \frac{\partial}{\partial \tau} E(\tau - t_0, \tau)\mathrm{d}\tau = H(t-t_0) \tag{25}$$

where $t_0 \geq 0$ and $H(t-t_0)$ is the Heaviside step function; $H(t-t_0) = 0$ and 1 for $t < t_0$ and $t > t_0$, respectively.

It will be helpful to use abbreviated notation for the hereditary integrals. For any function of time, f,

$$\{E\mathrm{d}f\} \equiv E_R^{-1} \int_0^t E(t-\tau, t) \frac{\partial f}{\partial \tau} \mathrm{d}\tau, \tag{26a}$$

$$\{D\mathrm{d}f\} \equiv E_R \int_0^t D(t-\tau, t) \frac{\partial f}{\partial \tau} \mathrm{d}\tau \tag{26b}$$

Also, in view of (23) and (24),

$$f = \{ E\mathrm{d}\{ D\mathrm{d} f \} \} = \{ D\mathrm{d}\{ E\mathrm{d} f \} \} \tag{26c}$$

Equations (23) and (24) become, respectively,

$$u_i^{\mathrm{R}} = \{ E\mathrm{d}u_i \}, \quad u_i = \{ D\mathrm{d}u_i^{\mathrm{R}} \} \tag{27}$$

Similar hereditary integrals are assumed to relate σ_{ij}^{R} and σ_{ij}, but modulus and compliance are interchanged,

$$\sigma_{ij}^{\mathrm{R}} = \{ D_1\mathrm{d}\sigma_{ij} \}, \quad \sigma_{ij} = \{ E_1\mathrm{d}\sigma_{ij}^{\mathrm{R}} \} \tag{28}$$

where the subscript 1 is used to indicate that the relaxation modulus and creep compliance (as well as another reference modulus $E_{\mathrm{R}1}$) are not necessarily the same quantities as in (27). Inasmuch as σ_{ij}^{R} and u_i^{R} are not in general the physical variables, we shall call them *pseudo stresses* and *pseudo displacements*, respectively. Similarly, the adjective pseudo will be used when referring to the potentials Φ, (3), Φ_{F}, (7), and Φ_{T}, (19), in the context of viscoelastic analysis.

The hereditary integrals used here are linear functionals with relaxation and creep functions which are independent of x_i. This behavior provides the useful property that differentiation with respect to x_i and hereditary integration may be interchanged; e.g.,

$$\partial u_i^{\mathrm{R}}/\partial x_j = \{ E\mathrm{d}(\partial u_i/\partial x_j) \}, \quad \partial u_i/\partial x_j = \{ D\mathrm{d}(\partial u_i^{\mathrm{R}}/\partial x_j) \} \tag{29}$$

The choice of constitutive equation (3), with pseudo and physical variables related in accordance with (27) and (28), is motivated by the fact that this constitutive theory approximates well the deformation behavior of various materials, and leads to relatively simple equations for viscoelastic deformation and fracture analysis. The latter point will be brought out in this paper. The validity of the constitutive theory has been discussed in [12,14,15] for the case in which $\sigma_{ij}^{\mathrm{R}} = \sigma_{ij}$. Observe that it reflects the commonly reported behavior in which stress-independent relaxation or creep functions in single integrals serve to characterize hereditary phenomena exhibited by many nonlinear materials. Also, some important special cases may be readily recovered through an appropriate choice of the material functions. Specifically, if $E = E_1 = D^{-1} = D_1^{-1} = E_{\mathrm{R}} = E_{\mathrm{R}1}$, (27) and (28) reduce to $u_i^{\mathrm{R}} = u_i$ and $\sigma_{ij}^{\mathrm{R}} = \sigma_{ij}$; consequently, (3) reduces to that for nonlinear elasticity. If $D_1^{-1} = E_1 = E_{\mathrm{R}1}$ and

$$D = (t_c E_{\mathrm{R}})^{-1}(t - \tau) \tag{30}$$

(where t_c is a time constant) we find $\sigma_{ij}^{\mathrm{R}} = \sigma_{ij}$ and

$$u_i^{\mathrm{R}} = t_c \partial u_i/\partial t \tag{31}$$

which, together with (3), yields linear or nonlinear viscous behavior. The general creep compliance $D = D(t - \tau, t)$, together with $\sigma_{ij}^{\mathrm{R}} = \sigma_{ij}$ (corresponding to $E_1 = E_{\mathrm{R}1}$) and a pseudo strain energy density which is proportional to that for a linear elastic, isotropic material in terms of $u_{i,j}^{\mathrm{R}}$, yields the standard constitutive theory for an aging linear viscoelastic material with constant Poisson's ratio; nonaging behavior results if $D = D(t - \tau)$. The generalization provided by (28) in which pseudo and actual stresses are not equal is useful for crack closing an healing analysis, as discussed later.

It should be mentioned that the notation $D = D(t, \tau)$ is employed in [14] instead of $D = D(t - \tau, t)$. These forms are equivalent, but the latter is more convenient in the study of crack growth. The pseudo energy Φ may also depend explicitly on time to account for effects of aging in the nonlinear behavior. "Aging" is not limited to intrinsic material changes, but may be due to direct physical causes such as transient temperatures and residual stresses [14].

4. Correspondence principles

Correspondence principles in linear viscoelasticity theory usually refer to elastic-viscoelastic relationships involving Laplace transformed stresses and displacements. Instead, here we shall give three correspondence principles for time-dependent, quasi-static solutions to nonlinear elastic and viscoelastic boundary value problems; they enable a viscoelastic solution to be easily constructed from an elastic solution. In terms of Piola stresses and coordinates x_i of B_0 the equilibrium equations are

$$\partial \sigma_{ij}/\partial x_j + F_i = 0. \tag{32}$$

The stress-pseudo displacement derivative equations,

$$\sigma_{ij} = \left\{ E_1 \mathrm{d}\left[\partial \Phi / \partial \left(u^{\mathrm{R}}_{i,j} \right)\right] \right\} \tag{33}$$

and body forces

$$F_i = -\left\{ E_1 \mathrm{d}\left(\partial \Phi_F / \partial u^{\mathrm{R}}_i\right) \right\} \tag{34}$$

in which

$$u^{\mathrm{R}}_{i,j} \equiv \left\{ E \mathrm{d}\left(\partial u_i / \partial x_j\right) \right\}, \quad u^{\mathrm{R}}_i \equiv \left\{ E \mathrm{d} u_i \right\} \tag{35}$$

lead to three intergro-differential field equations for the three displacements u_i when substituted into (32). The functions $\Phi = \Phi(u^{\mathrm{R}}_{i,j}, x_k, t)$ and $\Phi_{\mathrm{F}} = \Phi_{\mathrm{F}}(u^{\mathrm{R}}_i, x_k, t)$ are considered to be known; until Section 6, where the J_v integral is used, we allow for explicit dependence on all three coordinates x_k.

As boundary conditions we assume the traction potential $\Phi_{\mathrm{T}} = \Phi_{\mathrm{T}}(u^{\mathrm{R}}_i, x_k, t)$ is specified on a portion S_{T} of the surface; viz.,

$$\sigma_{ij} n_j = T_i \equiv -\left\{ E_1 \mathrm{d}\left(\partial \Phi_{\mathrm{T}} / \partial u^{\mathrm{R}}_i\right) \right\} \quad \text{on} \quad S_{\mathrm{T}} \tag{36}$$

Elsewhere, displacements $U_i = U_i(x_j, t)$ are given,

$$u_i = U_i \quad \text{on} \quad S_{\mathrm{U}}. \tag{37}$$

The total surface is $S = S_{\mathrm{T}} + S_{\mathrm{U}}$. Although not treated here, generalization of the analysis is easily made for mixed conditions in which different traction and displacement components are specified over the same part of the surface.

In all three correspondence principles the reference configurations B_0 of the elastic and viscoelastic bodies are specified to be identical (with identical cracks, if any). The first correspondence principle is restricted to time-independent surfaces:

CP-1. The viscoelastic solution (i.e., the stresses and displacements in the viscoelastic body which satisfy (32) (37)) is

$$\sigma_{ij} = \left\{ E_1 \mathrm{d} \sigma^{\mathrm{R}}_{ij} \right\}, \quad u_i = \left\{ D \mathrm{d} u^{\mathrm{R}}_i \right\} \tag{38}$$

where σ^{R}_{ij} and u^{R}_i satisfy equations of the reference elastic problem, (1), (3), (4), and (7), together with the boundary conditions,

$$\sigma^{\mathrm{R}}_{ij} n_j = T^{\mathrm{R}}_i \equiv -\partial \Phi_{\mathrm{T}} / \partial u^{\mathrm{R}}_i \quad \text{on} \quad S_{\mathrm{T}}, \tag{39a}$$

$$u^{\mathrm{R}}_i = U^{\mathrm{R}}_i \equiv \left\{ E \mathrm{d} U_i \right\} \quad \text{on} \quad S_{\mathrm{U}}. \tag{39b}$$

It is seen from (39b) that we first transform the given displacements U_i (if any) using the hereditary integral and obtain those needed in the elasticity problem. The governing equations of elasticity for the variables σ^{R}_{ij} and u^{R}_i are then solved. This solution is used in (38) to obtain the viscoelastic solution. That (38) is correct is easily established by

substituting it into (32)–(37). If the body forces F_i or surface tractions T_i are specified in the viscoelasticity problem, then one transforms them to obtain $F_i^R \equiv \{ D_1 dF_i \}$ and $T_i^R \equiv \{ D_1 dT_i \}$, after which the elasticity problem is solved using the potentials in (21).

When S_T and S_U vary with time certain difficulties arise. If $\partial n_i/\partial t \neq 0$ on S_T, then (39a) does not result in the correct condition, (36). This problem may be seen by observing that for the solution in (38),

$$\sigma_{ij} n_j = \left\{ E_1 d\sigma_{ij}^R \right\} n_j \neq \left\{ E_1 d\sigma_{ij}^R n_j \right\} \quad \text{on} \quad S_T \tag{40}$$

and therefore $\sigma_{ij} n_j \neq T_i$. Other difficulties are due to the effect of past values of T_i and U_i on current values of T_i^R and U_i^R. For example, consider $dS_T/dt > 0$ and Φ_T in (21). (By this shorthand notation we mean at least a portion of S_U becomes in time a surface on which T_i is given.) Then the traction T_i^R cannot be predicted for all $t > 0$ from the given boundary conditions on the part of S where the change from a displacement to traction condition occurs.

The next correspondence principle is for this type of boundary value problem, but we assume $E_1 = E_{R1}$. Hence, $\{ E_1 df \} = f$ for all functions f, and therefore the constitutive equation and body forces are, respectively,

$$\sigma_{ij} = \partial\Phi/\partial\left(u_{i,j}^R\right), \quad F_i = -\partial\Phi_F/\partial u_i^R. \tag{41}$$

Also,

$$\sigma_{ij} n_j = T_i \equiv -\partial\Phi_T/\partial u_i^R \quad \text{on} \quad S_T, \qquad u_i = U_i \quad \text{on} \quad S_U. \tag{42}$$

CP-II. If $dS_1/dt \geq 0$, the solution of viscoelastic equations (32), (35), (41), and (42) is

$$\sigma_{ij} = \sigma_{ij}^R, \quad u_i = \left\{ D du_i^R \right\} \tag{43}$$

where σ_{ij}^R and u_i^R satisfy the equations of the reference elastic problem, (1), (3), (4), and (7), together with the boundary conditions in (39) in which $T_i^R \equiv T_i$.

Verification of (43) is readily accomplished as before by substituting this solution into the governing viscoelasticity equations. Inasmuch as the elastic and viscoelastic stresses are the same throughout V and on S at all times, no basic difficulties arise in verifying the solution if $\partial n_i/\partial t \neq 0$ on S_1 and in determining T_i^R when (21) is used for Φ_T. However, the present class of problems obviously allows for crack growth, and certain physical questions of material continuity and interference have to be addressed. Pursuing this point, we observe that the relative displacement between crack faces, Δu_i, in the viscoelastic body is the difference of displacements in (43) evaluated on adjacent crack faces,

$$\Delta u_i = \left\{ D d\Delta u_i^R \right\} \tag{44}$$

where Δu_i^R is the displacement difference in the reference elastic problem. Since we have specified the instantaneous geometry of all cracks in the elastic problem to be the same as in the actual viscoelastic body, Δu_i is correctly predicted to vanish until the time t_1, say, when a crack tip reaches any particular physical location; this follows from the fact that $\Delta u_i^R = 0$ at this same location when $t < t_1$ (assuming prior cracking and rejoining of the crack faces has not occurred) which in turn implies the hereditary integral in (44) vanishes when $t < t_1$.

The present solution, (43), does not account for contact or rejoining of crack faces. Rather, it could predict that adjacent crack faces pass through one another if in the actual situation they rejoin and interfacial compression exists. Following such rejoining, the stresses in (43) are not valid, and the solution may become much more involved. We shall not consider the general problem here; rather, only the case in which cracks are initially

open and then close or shorten through a healing process is discussed. The third correspondence principle is concerned with the problem $dS_f/dt \leqslant 0$, and it is limited to the case $E = E_R$; (32)–(37) still apply except $u_i^R = u_i$ and $u_{i,j}^R = u_{i,j}$ are now used.

CP-III. If $dS_f/dt \leqslant 0$ and if $\partial n_i/\partial t = 0$ on S_f, the viscoelastic solution for the case $E = E_R$ is

$$\sigma_{ij} = \{ E_1 d\sigma_{ij}^R \}, \quad u_i = u_i^R \tag{45}$$

where σ_{ij}^R and u_i^R satisfy the equations of the reference elastic problem, (1), (3), (4), and (7), together with the traction boundary conditions (39a) and

$$u_i^R = U_i \quad \text{on} \quad S_U. \tag{46}$$

Verification of (45) is made as before. Observe that elastic and viscoelastic displacements are now equal, while the stresses depend on the relaxation modulus E_1. Also, it is of interest to observe that if tractions T_i are specified on crack surfaces (such as in the failure zone) the tractions T_i^R in the elastic problem are different from the actual values since $T_i^R = \{ D_1 dT_i \}$.

The Correspondence Principles II and III are not limited to crack problems. For instance, they may be applied to problems involving contact between different continua or ablation. Furthermore, even though they are based on apparently different constitutive equations they may in some cases be used for the same material, at least as an approximation. Indeed, for linear viscoelastic behavior in which the only effect of aging is in the relaxation moduli E and E_1 (i.e. Φ does not depend on time other than through the displacement derivatives), the two constitutive equations are easily shown to be equivalent if $E_1 = E$.

The remainder of this paper is concerned with crack growth analysis for materials obeying (41) and (42). The Correspondence Principle II (CP-II) and J_1 integral theory will be used in the development of criteria for predicting growth initiation time and crack speed.

5. Work input to the crack tip

An important quantity in crack growth analysis is the mechanical work available from the viscoelastic continuum for producing the separation (or at least a significant change of state) of material in the failure zone. This work, W_f, will be defined using an idealized model of the crack tip, and subsequently expressed in terms of the parameters J_f and J_1 of the reference elastic problem.

Consider as before a slender failure zone (in which α is large compared to the initial thickness of the failure zone in the x_2 direction) and locally two-dimensional deformations plus antiplane shearing. Before discussing W_f, let us recall that J_f for the elastic problem was defined through a line integral taken along the *instantaneous* interface between the continuum and failure zone. Furthermore, the surrounding material was assumed to obey (3), while no such restriction was imposed on the zone itself. For the present purposes of discussion, let us suppose this zone consists of the thinnest material layer for which (3) provides an adequate representation of the surrounding material. Figure 4 depicts the deformed failure zone (in the opening mode for simplicity) using a solid line to indicate the interface.

For the viscoelasticity problem, the work per unit undeformed area (in the x_1–x_3 plane) input by the continuum to a given material element (of width dx_1) in the failure zone from the time the crack tip arrives at the element, t_{i0}, to the time the left end of the

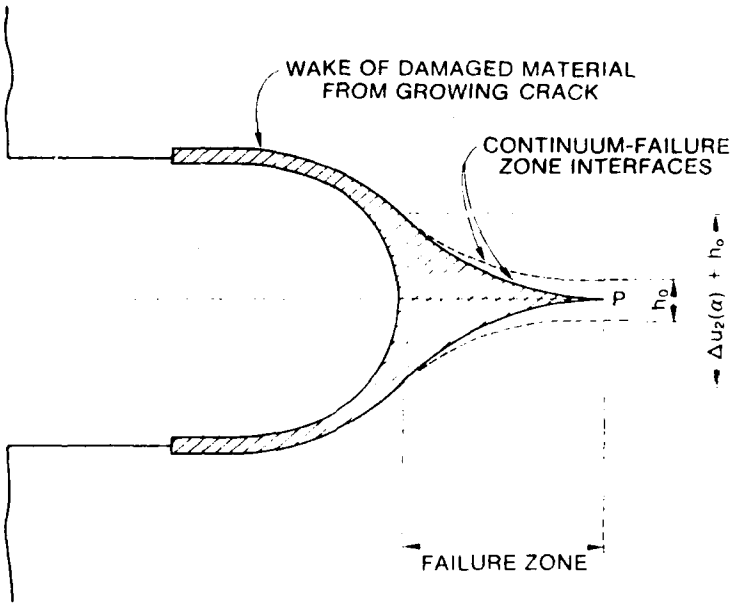

Figure 4. Deformed cross-section of crack in opening mode showing current interface between the continuum and all elements in the failure zone (———), and trajectory of the interface for the element currently at the left edge of this zone (- - - - - -).

failure zone arrives, t_α, is

$$W_f = \int_{t_\alpha}^{t} \tau_i \frac{\partial \Delta u_i}{\partial t} \mathrm{d}t. \tag{47}$$

The quantities τ_i and Δu_i $(i = 1, 2, 3)$ are Piola stresses and relative displacements, respectively, along the interface, and therefore they have the same significance as their counterparts in J_f, (9). Notice, however, that differentiation and integration in (47) is for a fixed value of x_1, whereas that in (9) is for a fixed time; thus, J_f does not in general reflect the deformation of a given material element. As a result, quite apart from the distinction between elastic and viscoelastic solutions, W_f is believed to be a more basic parameter than J_f for defining material failure.

There is an additional important difference between W_f and J_f as they have been introduced. Since W_f is the work input to one material element, the continuum-failure zone interface has to consist of the same continuum material points at $\xi = 0$ as at $\xi = \alpha$. The dashed line in Fig. 4 is intended to represent this interface. The height of the material element at $\xi = 0$ is indicated by h_0, which defines the thickness of the layer that ultimately becomes part of the failure zone; depending on the material behavior, the two interfaces may essentially coincide along a partial width or entire width $0 < \xi \leqslant \alpha$, or may not coincide until $\xi = \alpha$ $(t = t_\alpha)$. Considering the analysis to follow, in which Δu_i^R and Δu_i are to be related through CP-II, we should use the same material interface in the elastic and viscoelastic problems; the outer interface (the dashed line in Fig. 4) may be used if the undeformed value of h_0 is small enough to not invalidate (10). We shall assume that this is indeed the case.

According to CP-II, the relative displacements in the elastic and viscoelastic problems satisfy (44) if the tractions acting on the elastic and viscoelastic continua are the same.

(Recall that a traction potential Φ_f was used in the boundary conditions of CP-II (ref (42)); but it is clearly sufficient to use the same tractions, regardless of whether or not they are actually known or are expressed in terms of a potential.) Noting that stresses τ_i and τ_i^R are tractions along the continuum surface (apart from a sign change due to n_2), we specify $\tau_i^R = \tau_i$ in order to be able to use (44) in the next section. Criteria for the time t_i at which crack growth initiates and for the speed of propagation $\dot{a}$ will be studied.

6. Analysis of crack growth

Initiation of growth

For initiation we consider a material element which is at the left end of the failure zone $\xi = \alpha$ from $t = 0$ to t_i. As the body is loaded (beginning at $t = 0$) the crack tip P moves to the right but the element at $\xi = \alpha$ does not necessarily break immediately. Rather, it breaks at $t = t_i$, the so-called initiation time. We are interested in expressing the work input to this end element in terms of the far-field parameter J_v. In order to simplify the analysis so that viscoelastic effects may be shown clearly, stresses in the material in the failure zone will be idealized to those of a time-independent, rigid-plastic body; viz., we assume the τ_i are independent of t and ξ. Thus, from (9), (44), and (47),

$$J_f = \tau_i \Delta u_{i\alpha}^R \tag{48}$$

and

$$W_f = \tau_i \Delta u_{i\alpha} = \tau_i \{ D \mathrm{d} \Delta u_{i\alpha}^R \} = \{ D \mathrm{d} J_f \} \tag{49}$$

where $\Delta u_{i\alpha}^R$ and $\Delta u_{i\alpha}$ are the relative displacements at $\xi = \alpha$. The last result together with $J_v = J_f$, (10), and the notation in (26b), yields an explicit formula for work input at $t = t_i$:

$$W_f = E_R \int_0^{t_i} D(t_i - \tau, t_i) \frac{\mathrm{d} J_v}{\mathrm{d}\tau} \mathrm{d}\tau. \tag{50}$$

(See [12] for more general models of failure zone behavior.)

This result is the crack tip work per unit undeformed area in terms of two continuum-related parameters, J_v (which accounts for the geometry of B_0 and applied loads) and D, the creep compliance of the continuum. The J_v integral is the same as J for an elastic material when expressed in terms of the surface tractions. Also, just as for an elastic material, if the failure zone size α is small compared to all other geometric features, J_v is essentially independent of failure zone size and properties. Recall that E_R is a free constant, and may be selected as desired. (Its value does not actually affect W_f because J_v turns out to be inversely proportional to E_R.) Thus, if the continuum is elastic with a constant compliance D, we may use $E_R = D^{-1}$ and obtain the familiar result $W_f = J_v$.

An equation for predicting t_i is obtained by introducing the work $2\Gamma_i$ *required* to fail the element at $\xi = \alpha$. Thus (50) becomes

$$2\Gamma_i = \{ D \mathrm{d} J_v \}. \tag{51}$$

The factor of 2 is used because the "fracture initiation energy", Γ_i, is defined like a surface energy, counting the cross-sectional area of each side of the failed element at $\xi = \alpha$ as one unit of area. This energy is not necessarily a constant, even when the stress state of the crack tip is the same for all conditions of interest; as the failure zone displacement history may affect Γ_i. Whether Γ_i is a given constant or depends on $\Delta u_{i\alpha}$, (51) is an implicit equation for predicting t_i in terms of the history of J_v. On the other hand, one could use (51) to obtain Γ_i from tests of laboratory specimens by determining the value of the right hand side of (51) when the crack starts to grow under various test conditions, including different modes of crack tip deformation.

Finally, we observe that for the opening mode of crack tip deformation in a locally isotropic, linear viscoelastic material in plane strain,

$$J_\nu = (1 - \nu^2) K_I^2 / E_R \tag{52}$$

where K_I is the stress intensity factor and ν is the Poisson's ratio, assumed constant. (This familiar expression for linear materials may be derived from (9) and (10), for bounded stresses, by using [5, Part I (15) and (22)] for K_I and displacement.) Substitution of (52) into (51) to express the initiation criterion in terms of K_I yields the author's earlier result for linear viscoelasticity [5, Part II (64)].

Crack speed

Predictions of W_f for the next case with $\dot{a} > 0$ is facilitated by using ξ rather than t as the independent variable. Thus, (47) becomes

$$W_f = \int_0^\alpha \tau_i \frac{\partial \Delta u_i}{\partial \xi} d\xi \tag{53}$$

where $\Delta u_i = \Delta u_i(x_1, \xi)$. Equation (53) will be expressed in terms of J_ν for short-term steady state conditions. Namely, the speed $\dot{a}$ and failure zone length α are assumed to be essentially independent of time during a generic time interval $\alpha/\dot{a}$ for which the crack tip moves a distance α; during this same interval it is further assumed that τ_i and Δu_i are essentially independent of x_1 (although depending on ξ), α is small compared to the distance to other geometric features, and that there is no significant change in $D(t - \tau, t)$ due to aging (through the second argument, t).

These conditions, together with the observation from (44) that Δu_i and Δu_i^R are related in the same way as for a linear viscoelastic nonaging material, lead to the approximation [5, Part II],

$$\Delta u_i = E_R D(\tilde{t}, t) \Delta u_i^R \tag{54}$$

where $\tilde{t} \equiv k\xi/\dot{a}$. The factor k is a very weak function of slope $n \equiv \partial \log D / \partial \log \tilde{t}$, and is practically $1/3$ for the entire range of slopes ($0 \leqslant n \leqslant 1$) encountered in practice. Equation (54) and the value of k stem from the smooth, cusp-shaped relative displacement $\Delta u_i^R(\xi)$ predicted for a linear continuum (with bounded crack tip stresses), such as that illustrated in Fig. 2 for the opening displacement. Although further study of the accuracy of (54) seems warranted for nonlinear continua, it is likely to be a good approximation in many cases in view of the insensitivity of $\Delta u_i / \Delta u_i^R$ to the detailed behavior of $\Delta u_i^R(\xi)$ [5, Part II]; indeed, (54) may not require α to be small or constant.

Substituting (54) into (53) and using the same type of approximation as in the linear theory [5, Part II], which does *not* require τ_i to be spacewise constant, we find

$$W_f = E_R D(\tilde{t}_\alpha, t) \int_0^\alpha \tau_i \frac{\partial \Delta u_i^R}{\partial \xi} d\xi \tag{55}$$

where

$$\tilde{t}_\alpha \equiv k\alpha/\dot{a}. \tag{56}$$

The integration and differentiation in (55) is for x_1 fixed, while that in (9) is for t fixed (i.e., fixed crack tip location); however, because Δu_i^R and τ_i are independent x_1 (or t) for short-term steady-state growth, these integrals are equal. Equation (55) thus reduces to

$$W_f = E_R D(\tilde{t}_\alpha, t) J_f. \tag{57}$$

Upon equating W_f to the work *required* for failure of a material element, 2Γ, and using

(10) we obtain an implicit equation for $\dot{a}$,

$$2\Gamma = E_R D(\tilde{t}_a, t) J_v. \tag{58}$$

It should be recalled that the crack speed has been assumed constant for only the generic period $\alpha/\dot{a}$. Consequently, $\dot{a}$ as well as the other relevant parameters may vary over much longer periods without invalidating (58). Similar to the initiation problem, the linear theory [5, Part II] is recovered from (58) by using (52) for J_v. Also, for a linear viscoelastic material whose creep compliance obeys a power law in time, the factor k in (56) may be expressed exactly in terms of Gamma functions if the stress in the failure zone is spacewise constant [27, p. 118].

The failure zone may be viscoelastic, and therefore Γ could depend on $\dot{a}$ as well as other local parameters. After allowing also for possible dependence of α on J_v and $\dot{a}$, for proportional stressing (58) provides implicitly the functional relationship $\dot{a} = \dot{a}(J_v)$, as discussed in [12] and in the final subsection. The effect on $\dot{a}$ of the geometry of the undeformed body B_0 (in which crack lengths vary with time) and applied loads is entirely accounted for by the instantaneous value of J_v. In principle, a detailed model of the failure zone could provide this function; but if the effect of fundamental material parameters is not of concern, one would normally determine $\dot{a}(J_v)$ experimentally.

Effect of a process zone or interlayer on crack speed

Figure 5 shows a failure zone within a "process zone" of length β. The latter zone is introduced in part to account explicitly for the fact that with some materials, especially plastics, there is a zone around the crack tip which has different viscoelastic properties than the surrounding continuum [e.g., 13]. Also, Fig. 5 can be interpreted as a model for crack growth in an adhesive layer, in which the adjacent continuum represents the two elastic or viscoelastic adherends. Besides these uses, we may consider the process zone to be a failure zone as previously defined (but now with some limitations on its constitutive properties), and thereby obtain detailed information on Γ from the subsequent analysis.

For the class of damageable materials introduced in the Appendix, a pseudo strain energy density Φ exists for the response to both loading and unloading. Additionally, J_v is independent of path under many conditions. We shall assume one path-independent

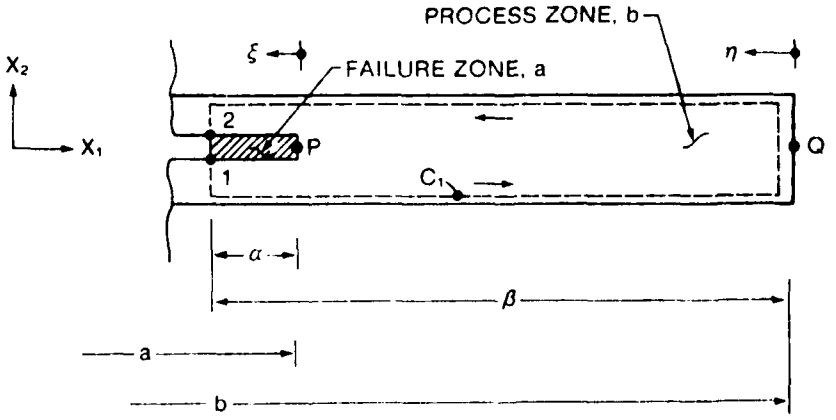

Figure 5. Cross-section of crack in undeformed body with crack tip P embedded in material layer (process zone) having deformation characteristics different from surrounding continuum. The failure zone is not necessarily centered.

integral exists for the process zone, and another exists for the surrounding continuum. The creep compliances and Φ for the two regions may be different, and therefore these integrals are not necessarily equal.

Local two-dimensional deformations, appropriate to the use of (12) for the process zone, are assumed. Furthermore, C_1, is now taken to be the dashed line in Fig. 5, which is adjacent to the continuum-process zone interface. Subscripts "a" and "b" will be used when necessary to distinguish between quantities for the failure zone and process zone, respectively. A letter subscript will not be used with parameters of the continuum.

The process zone is assumed to be thin in the x_2 direction (relative to β) so that arguments similar to those given previously for the failure zone may be employed; this slenderness greatly simplifies the analysis while the essential physical features are retained. Thus, (10) is used,

$$J_x = J_{fb} \tag{59}$$

where J_x is in (11) and (cf. Fig. 5),

$$J_{fb} = \int_0^{\beta} \tau_i \frac{\partial \Delta u_i^R}{\partial \eta} \mathrm{d}\eta \tag{60}$$

Similarly, for the J integral in the process zone,

$$J_{xb} = J_{fa} \tag{61}$$

where

$$J_{fa} = \int_0^{\alpha} \tau_{ib} \frac{\partial \Delta u_{ib}^R}{\partial \xi} \mathrm{d}\xi. \tag{62}$$

It is important to recognize that in using (59) (62) we are, in effect, neglecting the contribution of the vertical segments at P and Q, Fig. 5, to the integral in (8) for each contour. The other simplification employed is that the Piola stresses along the top horizontal line of each contour equal those along the bottom. The same simplifying features are assumed to apply to J_{xb} when evaluated on C_1; thus, (12) yields

$$J_{xb} = \int_0^{\beta} \tau_{ib} \frac{\partial \Delta u_{ib}^R}{\partial \eta} \mathrm{d}\eta + I_a \tag{63}$$

where I_a is the integral along the vertical segment below point 1 and above point 2 in Fig. 5. This contribution is retained even though the integral along the vertical path at Q (within the process zone) is neglected. The difference is due to the value of Φ_b at $\xi = \alpha$, which may be very large as a result of damage in the process zone (cf. Appendix), while Φ_b at $\eta = 0$ will be small if $|\partial u_{ib}^R/\partial x_1|$ is small; the contribution of the integral of $T_{ib}\partial u_{ib}^R/\partial x_1$ on the vertical lines is considered to be negligible due to, for example, smallness of $|\partial u_{ib}^R/\partial x_1|$ at $\eta = 0$ and $|T_{ib}|$ at $\xi = \alpha$ or the slenderness of the process zone. Considering the fact that the vertical paths at Q in the process zone and the continuum have been neglected and recalling conditions for which $d = 0$, we are, in effect, defining Q to be close to or ahead of the leading edge of major softening processes and to straddle the location where the creep compliance D and function Φ (for the continuum) change to D_b and Φ_b, respectively (for the process zone); of course, if $D = D_b$ and $\Phi = \Phi_b$, the latter constraint is not involved. The distance over which the change in functions occurs should be small compared to β or at least be such that the result of interest, (73), is not sensitive to the physical location selected or calculated for Q.

Approximations like that in (54) will be used to evaluate the viscoelastic displacement. Thus, for the continuum just outside the process zone,

$$\Delta u_i \doteq E_R D(\tilde{t}, t) \Delta u_i^R, \quad \tilde{t} = k\eta/a \tag{64}$$

the process zone just inside the continuum,

$$\Delta u_{ib} = E_R D_b(\tilde{t}_b, t)\Delta u_{ib}^R, \quad \tilde{t}_b \equiv k_b\eta/\dot{a} \tag{65}$$

and the process zone just outside the failure zone,

$$\Delta u_{ib} = E_R D_b(\tilde{t}_a, t)\Delta u_{ib}^R, \quad \tilde{t}_a \equiv k_a\xi/\dot{a}. \tag{66}$$

In view of the local steady-state assumption implicit in these approximations, $\dot{a} = \dot{b}$; also, because E_{Rb} and E_R are free constants, we have used $E_{Rb} = E_R$.

Let us next relate J_{vb} to J_v. This may be done by using the continuity of displacements and normal and shearing stresses across the continuum-process zone interface: $\Delta u = \Delta u_{ib}$ and $\tau_i = \tau_{ib}$. The first condition together with (64) and (65) yields

$$\Delta u_{ib}^R = \frac{D(\tilde{t}, t)}{D_b(\tilde{t}_b, t)}\Delta u_i^R. \tag{67}$$

Substitute this result into (63), use the same type of approximation that lead from (53) to (55) (but now with the D-ratio in (67) entering in place of D in (54)), and then employ (59) and (60). There results, finally,

$$J_{vb} = \frac{D(\tilde{t}_\beta, t)}{D_b(\tilde{t}_{b\beta}, t)}J_v + I_a \tag{68}$$

where

$$\tilde{t}_\beta \equiv k\beta/\dot{a}, \tilde{t}_{b\beta} \equiv k_b\beta/\dot{a} \tag{69}$$

and approximately $k \simeq k_b = 1/3$. Additionally (cf. Appendix),

$$I_a \equiv -\int_a \Phi_b dx_2 \tag{70}$$

where the integral is taken upward along the vertical lines at $\xi = a$; on the basis of the physical significance of Φ_b we have $I_a \leqslant 0$, where $I_a = 0$ when there is no damage in the process zone. It should be observed that we have neglected the contribution from the body force potential because of the slenderness of the process zone.

The work input to the failure zone is given by (57) after replacing D by D_b, J_f by J_{fa}, (62), and then using (61) and (68),

$$W_f = E_R D_b(\tilde{t}_a, t)\left[\frac{D(\tilde{t}_\beta, t)}{D_b(\tilde{t}_{b\beta}, t)}J_v - \int_a \Phi_b dx_2\right] \tag{71}$$

where

$$\tilde{t}_a \equiv k_a\alpha/\dot{a}, \quad k_a \simeq 1/3. \tag{72}$$

Equating W_f to the work required for rupture of an element of unit area in the failure zone, 2Γ, we find the implicit equation for $\dot{a}$,

$$2\Gamma_b = E_R D(\tilde{t}_\beta, t)J_v \tag{73}$$

where

$$2\Gamma_b \equiv \left[\frac{2\Gamma}{E_R D_b(\tilde{t}_a, t)} + \int_a \Phi_b dx_2\right]E_R D_b(\tilde{t}_{b\beta}, t). \tag{74}$$

The quantity Γ_b is the "fracture energy" of the process zone; it is introduced in order to write the crack speed relation, (73), in the same form as (58) for the failure zone alone; Γ_b consists of the failure zone energy Γ, the work of damage (given by the integral in (74)),

and the "local" creep compliance D_b in terms of two local times, $\tilde{t}_a$ and $\tilde{t}_{b\beta}$.

As a result of damage in the process zone, the fracture energy Γ may be negligible (or, equivalently, the failure zone may not exist). Equation (74) then reduces to

$$2\Gamma_b = E_R D_b(\tilde{t}_{b\beta}, t) \int_a \Phi_b \mathrm{d}x_2 \tag{75}$$

which is to be substituted into (73) to obtain the equation for $\dot{b}(\equiv \dot{a})$. This result corresponds to using $J_{vb} = 0$ in (68).

If W_f in (71) is negative, i.e.,

$$J_v < \frac{D_b(\tilde{t}_{b\beta}, t)}{D(\tilde{t}_\beta, t)} \int_a \Phi_b \mathrm{d}x_2 \tag{76}$$

there is insufficient mechanical work available to break material elements in the process zone. In this case, the crack will not propagate or, at least, quasi-static steady-state propagation cannot exist. Even if $W_f > 0$, steady-state propagation may not exist when (73) predicts $\mathrm{d}J_v/\mathrm{d}\dot{a} < 0$. An examination of (73) indicates this situation is a physical possibility without having to consider dependence of α, β, Γ, and Φ_b on $\dot{a}$. For example, suppose $\int \Phi_b = 0$, $DE_R = 1$ and that α, β, and Γ are independent of $\dot{a}$. Also, let $k = k_a = k_b$ so that $\tilde{t}_\beta = \tilde{t}_{b\beta} = k\beta/\dot{a}$ and $\tilde{t}_\alpha = k\alpha/\dot{a}$. Equations (73) and (74) yield

$$\frac{2\Gamma D_b(\tilde{t}_\beta, t)}{D_b(\alpha\tilde{t}_\beta/\beta, t)} = J_v. \tag{77}$$

It is helpful to express the derivative of J_v using logarithms,

$$-n_b + n_a = \mathrm{d}\log J_v/\mathrm{d}\log \dot{a} \tag{78}$$

where

$$n_b \equiv \frac{\partial \log D_b(s, t)}{\partial \log s} \qquad \text{at} \quad s = \tilde{t}_\beta \tag{79}$$

and

$$n_a \equiv \frac{\partial \log D_b(s, t)}{\partial \log s} \qquad \text{at} \quad s = \alpha\tilde{t}_\beta/\beta \tag{80}$$

are logarithmic slopes of the creep compliance curve (for a fixed age t) at a creep time of $s = \tilde{t}_\beta$ and the shorter creep time $s = \alpha\tilde{t}_\beta/\beta$. For real materials $(n_a, n_b) \geq 0$. Also $n_a < n_b$ if s is sufficiently small; in this case, $\mathrm{d}J_v/\mathrm{d}\dot{a} < 0$. For many materials $n_a > n_b$ at long creep times s, and thus $\mathrm{d}J_v/\mathrm{d}\dot{a} > 0$; the function $J_v(\dot{a})$ is therefore predicted to have a maximum at an intermediate crack speed.

Prediction of process and failure zone sizes

The lengths β and α which appear in the argument of creep compliance in the equations for crack speed are not necessarily constant. In fact they are related through (59) and (61), respectively, to the J_v integrals and to a measure of the stress in the two zones. In [12] it was noted that for the failure zone alone the condition $J_v = J_f$ leads to such a relationship, which in turn reduces to that derived earlier for a small-scale failure zone in linear viscoelastic media using Barenblatt's condition for finite crack tip stresses [5, Part I]. Equations (59) and (61) are for slender zones, but β and α may be large and the material may be nonlinear, viscoelastic, and anisotropic.

Mechanical state solutions, including zone size, were derived in [12] for a failure zone in

a power law material. Here, we use the same approach to derive β and α. Consider, for example, the use of (59) and the power law potential (a so-called homogeneous function of degree $M+1$),

$$\Phi(cu_{i,j}^{R}) = |c|^{M+1}\Phi(u_{i,j}^{R}) \tag{81}$$

to obtain an expression for β. The result is (cf. derivation of (39) in [12]),

$$\beta = \left|\frac{\sigma_0}{\sigma_b}\right|^{1/M}\frac{J_x}{|\sigma_b|I_1} \tag{82}$$

where σ_b and σ_0 have dimensions of stress and are independent of x_1, but may vary with t, $\dot{a}$, etc.; they are introduced to express the interface stresses τ_i and potential Φ in terms of dimensionless functions f_i and Φ_M.

$$\tau_i = \sigma_b f_i, \quad \Phi = \sigma_0\Phi_M. \tag{83}$$

Also, $|\ |$ denotes absolute value and

$$I_1 \equiv \int_0^1 (\partial g_i/\partial z) f_i \,\mathrm{d}z \tag{84}$$

where $z \equiv \eta/\beta$, and g_i are dimensionless interface displacements,

$$g_i \equiv \mathrm{sign}(\sigma_b)|\sigma_0/\sigma_b|^{1/M}\Delta u_i^{R}/\beta. \tag{85}$$

As in [12], it can be shown that under certain conditions I_1 is a constant (apart from parameters which appear in Φ_M, such as M and aging time t); although linear strain-displacement relations were used previously, the form of the mechanical state solutions and the conditions are unaffected by the magnitude of the strains if the power law, (81), is applicable. These conditions are: (i) the "shape factor" for interface tractions is given as $f_i = f_i(z, g_j)$ where $z \equiv \eta/\beta$; (ii) the continuum is locally homogeneous (i.e. Φ_M is independent of x_1, other than through $\partial u_i^{R}/\partial x_1$); (iii) the process zone size β is small compared to the distance to geometric features outside of the zone; (iv) the crack faces are locally traction free, apart from the interface tractions τ_i. Without further analysis one cannot quantify "local" and say how small β must be. However, it may be necessary for there to be a neighborhood of the crack tip on the order of 10^2–100β in which conditions (ii)–(iv) are met. The process zone must be small enough that the remote stress field is essentially the singular solution $\sigma_{ij}^{R} \sim r^{-M/(M+1)}$, where r is the distance (in the x_1–x_2 plane) to the crack tip. Condition (iv) may be relaxed to allow for spacewise uniform tractions on a linear continuum and spacewise uniform normal tractions on an incompressible, nonlinear continuum; the extension is achieved through superposition of a uniform stress field. Also, if $f_i = f_i(z, g_j, \dot{a}, J_x, \alpha)$ in condition (i), then $I_1 = I_1(\dot{a}, J_x, \alpha)$.

The analysis in [12] is for the opening mode of crack tip deformation. However, the form of the results is the same for other modes, including mixed-mode deformation. One may then argue by analogy that I_1 is constant under the same conditions as stated in [12] if proportional stressing exists; i.e., if the ratio of stresses in the remote singular stress field is independent of time.

For uniaxial stress σ_{11}^{R}-strain $u_{1,1}^{R}$ behavior, (81) implies $|u_{1,1}^{R}|^{1/M} \sim |\sigma_{11}^{R}|\,\sigma_0^{-(1+M)/M}$. Thus, if $M \gg 1$, σ_0 may be interpreted as a yield stress; if $M = 1$, σ_0 is a modulus. Equation (82) in turn provides the relation between σ_0, a measure of the intrinsic strength of the process zone σ_b, and a measure of the external loading J_x. If the process zone is also a power law material (in the neighborhood of the failure zone) with nonlinear exponent M, a similar analysis yields

$$\alpha = \left|\frac{\sigma_{0b}}{\sigma_a}\right|^{1/M}\frac{J_{xb}}{|\sigma_a|I_{1a}} \tag{86}$$

where the parameters are analogous to those in (82). If, however, there is considerable nonuniformly distributed damage surrounding the failure zone, it is not likely that a power law nonlinearity with a single exponent $\hat{M}$ will be a good representation.

J_v as a characterizing parameter

Consider again a power law nonlinear material with a small scale process zone, in which the damage and failure behavior of material elements is unaffected by stresses and deformations prior to the arrival of the tip Q, Fig. 5. Further, assume J_v and $\dot{b}(=\dot{a})$ are essentially constant during the time $\beta/\dot{a}$ required for the process zone to propagate its length. The state of stress in the remote continuum where the aforementioned singular solution applies is determined solely by the current value of J_v for proportional stressing, just as for an elastic material. This dependence implies J_v is the only remove field parameter which affects Δu_i^R; the process zone characteristics of course affect Δu_i^R. From (64) we see that the same conclusion applies to the viscoelastic displacement, Δu_i, except crack speed now appears. The damage and failure parameters α, β, Γ, and $f\Phi_b$ in (73) and (74) may not be constant, but any variation will be due to J_v and $\dot{a}$ (e.g. (82)), apart from aging or environmental parameters such as the external temperature. (Local temperature changes due to mechanical deformation are determined similarly by J_v and $\dot{a}$.) Equation (73) therefore serves to define the function $\dot{a} = \dot{a}(J_v)$, indicating that J_v is the "characterizing parameter" for crack speed. In principle, this function could be obtained experimentally through measurements of speed. However, by introducing specific models for behavior of the process and failure zones, one could use (73) to relate crack speed to material parameters as well as J_v. Elementary examples are given in [12] for a failure zone in a continuum obeying a power law with respect to both time (through the creep compliance) and strain: the relation $\dot{a} \sim J^{k'}$ is derived, where k' is a simple function of both exponents which depends on characteristics of the failure zone. The assumption of an "elastic-like" failure zone for opening mode propagation (Γ and τ_f independent of speed) was shown in [5, Part III] to provide a function $\dot{a} = \dot{a}(J_v)$ which agreed well with experimental data on a crosslinked rubber; in this study there was no process zone and the continuum was linearly viscoelastic (cf. (52)). See also [7,20,21] for linear behavior.

The J_v integral may serve as the characterizing parameter for initiation time or crack speed when some of the previously stated conditions (e.g. small-scale crack-tip zone) are not met, depending on characteristics of the process and failure zones. An example was given earlier for initiation time, (51), in which α was not restricted in size. However, further experimental and theoretical studies are needed to establish the necessary conditions.

7. Concluding remarks

Methods of quasi-static deformation and fracture analysis have been developed for nonlinear viscoelastic media. The correspondence principles which provide the basis for the analysis are not limited to crack growth; they apply to crack closing and healing as well as to other types of problems involving ablation and interfacial contact and separation. However, only crack growth examples are given.

Constitutive equations

Nonlinear effects in Eqn. (41) for stresses are characterized by a potential Φ which is analogous to strain energy density. This pseudo energy is expressed in terms of the history of displacement derivatives through Eqn. (23), rather than the history of Green's strains.

and therefore material objectivity may not be satisfied when large deformations exist; i.e., depending on the deformation history and material type, Φ could be affected by rigid rotations. Material objectivity can always be satisfied when linear strain-displacement equations are applicable. In this case, one would express Φ as a function of displacement derivative history through the strain history [12].

A single hereditary integral, (23), is used in (41) to account for viscoelastic effects, and therefore some details of the complex stress-deformation behavior of many materials may not be followed. However, the theory does contain general material-objective representations of the important cases of nonlinear elastic and viscous media under small or large deformations and the common type of linear viscoelastic material which is characterized by one independent relaxation or creep function. In certain problems of crack growth in linear viscoelastic orthotropic materials, the several independent creep functions combine into just one function for predicting load-displacement response of the crack plane [8]. This feature enables us to generalize (58) and (73) for crack tip work by simply replacing D with this group of creep compliances.

For large deformations of viscous materials, the current geometry would be considered the "undeformed" state B_0 in order to recover the classical constitutive equations [17]; the basic expression for relating crack tip and far-field behavior, (10), is not invalidated in this case if the opening displacement Δu_2 along the failure zone, Fig. 1, or process zone, Fig. 5, is small compared to the length α or β, respectively. On the other hand, this condition of a slender crack-tip zone in the *current* geometry is not needed for an elastic material.

As discussed in other work [12,14], the nonlinear viscoelastic constitutive equations used here in the fracture theory may be written in the form of a special type of a so-called modified superposition principle employed successfully with polymers and metals [e.g. 15, 19]. We have introduced effects of aging and microstructural changes (e.g. damage) in the standard modified superposition principle. This "aging" is not limited to independent physical or chemical processes, and may be used to account for differences in nonlinear behavior at short and long times and, as shown in the Appendix, to account for damage characterized by Lebesgue norms of deformation-related parameters.

In view of these extensions of the standard single-integral representation for hereditary behavior, and the important limiting cases contained in the theory (including specific microcracking models and deformation theory of plasticity with elastic unloading), it is believed the constitutive equations are sufficiently general to account for the primary features, if not all details of actual deformation behavior, of a wide variety of materials. Nevertheless, considerable additional study is needed to establish the range of validity of the equations for different materials and conditions. For example, it would be interesting to determine for rubber the accuracy of the stress-deformation relation in (41), which is similar to the theory developed and successfully applied to rubber by Tschoegl and coworkers [22].

The "pseudo displacements", u_i^R, which appear in (41) and (43), are related to the physical displacements u_i through the hereditary integral, (23). If the constitutive theory is valid for global response, the material behaves overall as an elastic body when loads or stresses are expressed in terms of pseudo displacements; as illustrated in [15], this type of behavior for nonaging materials with constant damage may be easily checked by converting experimentally measured displacements to pseudo displacements through (23) and then examining measured load-pseudo displacement diagrams.

Crack growth

Considering the complex states of deformation and damage around real crack tips, indirect determination of specific constitutive equations using specimens with stationary

and propagating cracks may be an important complement to studies of specimens under homogeneous deformation histories. This determination would be aided by the simple relation between elastic and viscoelastic displacements, (43), and the fact that (41) for stresses, including the generalization in the Appendix, leads to relatively simple equations for crack growth, (51), (58), and (73).

The quantity J_v in these equations has a very simple meaning in certain cases. If hereditary behavior of the entire continuum outside of the process and failure zones can be represented by the one creep compliance D (or relaxation modulus E), the J_v is the same as the familiar J integral for nonlinear elastic materials and C^* for viscous materials when expressed in terms of externally applied loads (rather than displacements). The pseudo potential energy P_v, (18), is related similarly to the potential energy for elastic media. If $u_i \simeq u_i^R$, except possibly for a small neighborhood or crack tips, J_v and $-\partial P_v/\partial A$ are essentially the elastic J integral and energy release rate, respectively. The ratio $2\Gamma/E_R D$ from (58), or $2\Gamma_b/E_R D$, (73), then appears as the fracture energy for an elastic material if $J_v = -\partial P_v/\partial A$; this "apparent fracture energy" may depend on crack speed through D, Γ, or Γ_b. For the rubber studied in [5, Part III], all effects of speed come through the nonaging form of compliance, $D = D(\tilde{t}_a)$. For a viscous body, C^* is approximately three times the length-averaged power input per unit area to the failure zone during short-term steady state propagation if we use $\tau_v = 1$ in (30) [12]; it can be shown that the factor is exactly three for a linear viscous material if the stress in the failure zone is spacewise constant.

Direction of crack growth

Prediction of the direction of crack growth has not yet been discussed in this paper. Many of the relationships hold whether or not the direction changes, but the problem is too complex to treat here in any detail. We would only suggest a possible approach. Referring to Fig. 3, suppose for purposes of discussion the local coordinate axis is fixed and various relative orientations θ for the continuum are considered. The actual θ's for initiation and continuation of growth may correspond to the predicted directions for which t_i is a minimum and $\dot{a}$ is a maximum, respectively. These criteria automatically account for local and global material anisotropy through the variation of values of the material and loading parameters (such as Γ, α, and J_v in (58)) with respect to θ. Also, these proposed criteria reduce to the well-established one of maximum energy release rate for crack growth in an elastic isotropic body. The equations for crack speed have been derived under the simplifying condition of short-term steady state behavior; with crack tip reorientation it is likely that the equations will remain valid if θ is small in magnitude and essentially constant for an amount of growth equal to the length α or β of the crack tip zone.

Crack tip models

Emphasis of the fracture analysis in this paper has been on predicting the mechanical work available at the crack tip for initiation and continuation of growth. The right-hand side of (58) and (73) is this work at the failure zone (without a process zone) and process zone edges, respectively. By assuming the theory in the Appendix is valid for the process zone, we have obtained some information on how the creep compliance D_b and pseudo energy Φ_b of the process zone affect the required work $2\Gamma_b$, (74). Viscoelastic behavior of the embedded failure zone in Fig. 5 is reflected in the value of Γ, and it may be different from that of the process zone and continuum. Because the process zone is slender, we were able to obtain a relatively simple relationship, (68), between its J_v integral, J_{vb}, and J_v for the surrounding continuum (or the adherends, in the case the process zone is actually a

thin adhesive interlayer). Also, it should be observed that (71) for available work allows for distributed damage outside the process zone as long as the theory in the Appendix applies. This feature is important for many materials, especially composites.

With the dual crack tip zones, Fig. 5, one can account for a distinct, complex material separation zone (α) within a relatively well-defined layer of damaged material (β). This geometry may be a realistic model of the delamination tip region in fibrous composites with rubber-toughened matrices [23, Fig. 3] and a cracked craze layer in plastics. As a special case the failure zone could be omitted; one may interpret this situation as the original one in which only a failure zone exists, (58), but with an explicit viscoelastic representation for the fracture energy. As shown in [5, Part III] this energy for rubber may be independent of crack speed. When this is true, the molecular theory for fracture energy of rubber in its elastic range [2] serves to relate Γ_b to molecular parameters, and (73) brings in the only viscoelastic effects through D; the notch-tip diameter (≈ 50 Å) used in [2] is to be associated with the process zone height in the undeformed state.

It is believed the theory in this paper will be helpful in developing detailed crack tip models which relate growth behavior directly to local physical, chemical, and mechanical processes; a possible general approach would consist of using the available crack tip work, (71), in a local nonequilibrium thermodynamic formulation for the process and failure zones. Much of the published work on crack tip models employs the classical singular solutions for the local mechanical state. However, whether propagation is continuous or occurs in steps [e.g. 24, 25], use of continuum mechanics and thermodynamics with bounded stresses should lead to more direct relationships between basic material parameters and crack growth, as illustrated here.

Acknowledgment

The au[illegible] is grateful to the U.S. Air Force Office of Scientific Research, Office of Aerospace Research (with Major David Glasgow as Program Manager) for sponsoring this research, and to Mr. J.R. Weatherby, graduate research assistant, for his review of the manuscript and helpful comments.

References

[1] D. Broek, *Elementary Engineering Fracture Mechanics*, Third revised edn., Martinus Nijhoff Publishers (1982).
[2] G.J. Lake, in *Progress of Rubber Technology*, Applied Science Publishers Ltd. (1983) 89-143.
[3] J.R. Rice, *Journal of Applied Mechanics* 35 (1968) 379-386.
[4] J.D. Landes and J.A. Begley, in *Mechanics of Crack Growth*, ASTM STP 590, American Society for Testing and Materials (1976) 128-148.
[5] R.A. Schapery, *International Journal of Fracture* 11 (1975): Part I, 141-159; Part II, 369-388; Part III, 549-562.
[6] A.A. Kaminskii, *Prikladnaya Mekhanika* 16 (1980) (English translation (1981) Plenum) 3-26.
[7] R.M. Christensen, *Theory of Viscoelasticity, An Introduction*, Second edn., Academic Press (1982).
[8] C.S. Brockway and R.A. Schapery, *Engineering Fracture Mechanics* 10 (1978) 453-468.
[9] R.A. Schapery, *International Journal of Fracture* 14 (1978) 293-309.
[10] F.H.K. Chen and R.T. Shield, *Journal of Applied Mathematics and Physics ZAMP*, 28 (1977) 1-22.
[11] R.T. Shield, in *Finite Elasticity*, R.S. Rivlin Ed., The American Society of Mechanical Engineers (1977) 1-10.
[12] R.A. Schapery, in *Encyclopedia of Materials Science and Engineering*, Pergamon Press LTD (1986) (To appear).
[13] E. Passaglia, *Polymer* 23 (1982) 754-760.
[14] R.A. Schapery, in *1981 Advances in Aerospace Structures and Materials*, S.S. Wang and W.J. Renton, Eds., The American Society of Mechanical Engineers (1981) 5-20.
[15] R.A. Schapery, in *Proceedings Ninth U.S. National Congress of Applied Mechanics*, The American Society of Mechanical Engineers (1982) 237-245.

[16] J.K. Knowles and E. Sternberg, *Archive for Rational Mechanics and Analysis* 44 (1972) 187-211
[17] Y.C. Fung, *Foundations of Solid Mechanics*, Prentice-Hall, Inc. (1965).
[18] M.D. Greenberg, *Foundations of Applied Mathematics*, Prentice-Hall, Inc. (1978).
[19] W.N. Findley, *Journal of Applied Mechanics* 48 (1981) 47-54.
[20] W.G. Knauss, in *Deformation and Fracture of High Polymers*, H. Henning Kausch, John A. Hassell and Robert I. Jaffee, (eds.), Plenum Press (1974) 501-541.
[21] L.N. McCartney, *International Journal of Fracture* 15 (1979) 31-40.
[22] N.W. Tschoegl, *Polymer* 20 (1979) 1365-1370.
[23] W.L. Bradley and R.N. Cohen, in *Proceedings Fourth International Conference on Mechanical Behavior of Materials*, J. Carlsson and N.G. Ohlson, Pergamon Press (1983) 595–604.
[24] R.W. Hertzberg and J.A. Manson, in *Fatigue of Engineering Plastics*, Academic Press (1980) 160.
[25] A.J. Kinloch, *Metal Science* (1980) 305-318.
[26] L.E. Malvern, *Introduction to the Mechanics of a Continuous Medium*, Prentice-hall, Inc. (1969).
[27] J.G. Williams, *Fracture Mechanics of Polymers*, Halstead Press, John Wiley & Sons (1984).

Appendix

Effect of time-varying microstructural changes

Certain important inelastic effects, besides those represented by the creep compliance, can be taken into account in the J_x integral theory. These additional effects are associated with "distributed damage" or, what may be a better term, "microstructural changes". Special cases are microcracking, dislocation motion and generation, hole growth, and breaking of entanglement points along polymer chains. Here, we propose a theory of inelastic behavior, allowing for large deformations. The formulation is in terms of the *reference problem*, which is the reference elastic problem with damage; the viscoelastic variables are still related to those for the reference problem through (27) and (28). For lack of a better short name, we are using "damage" when referring to changes in the microstructure or fabric of a material. However, the specific "damaging process' does not have to be identified here; it could include healing (decrease in damage) as well as other changes which are beneficial to structural performance.

Constitutive theory

It is assumed on physical grounds that a strain energy potential exists when the damage is constant (for instance, during unloading without significant interfacial friction following development of microcracking in a composite or following plastic deformation in a metal). Denoting this potential by Φ^{C}, for reasons to be given we assume it has the form

$$\Phi^{\mathrm{C}} = \Phi_0\left(u^{\mathrm{R}}_{i,j}, x_k, t\right) + \sum_{n=1}^{\Lambda} \Phi_n\left(I_{n_1}, I_{n_2}, x_k, t\right). \tag{A.1}$$

The $u^{\mathrm{R}}_{i,j}$ enter Φ_n through the functions $I_{n_\alpha} = I_{n_\alpha}(u^{\mathrm{R}}_{i,j})$; as a special case, I_n may be a strain or a strain invariant. We further assume that *all* of the functions are smooth enough to permit the various mathematical operations which are performed. The Φ's may depend on x_k and t, as indicated, but this material nonhomogeneity and aging will not be explicitly shown in subsequent work unless needed for clarity. Also, throughout the Appendix summation over n is not intended unless $\sum$ is used.

By definition, all quantities I_{n_α} (which will be called *damage parameters*) are constant during a constant damage process. In this case (3) and (A.1) yield the Piola stresses,

$$\sigma^{\mathrm{R}}_{ij} = \frac{\partial \Phi_0}{\partial\left(u^{\mathrm{R}}_{i,j}\right)} + \sum_{n=1}^{\Lambda} \frac{\partial \Phi_n}{\partial I_{n_\alpha}} \frac{\partial I_{n_\alpha}}{\partial\left(u^{\mathrm{R}}_{i,j}\right)} \tag{A.2}$$

By further definition, the only other process which can occur is called a *damaging process* and is such that $I_{n_\alpha} \le I_{n_\alpha}$ for *all* parameters I_{n_α}; at the end of this Appendix a simple generalization will be made in which $I_{n_\alpha} > I_{n_\alpha}$ for some of the damage parameters. It is assumed that the stresses are continuous in the displacement derivatives, and therefore (A.2) defines the stresses with constant or varying damage.

The formulation for constant damage may be visualized very easily by considering a uniaxial stress $\sigma(=\sigma^{\mathrm{R}}_{11})$-strain $\epsilon(=\partial u^{\mathrm{R}}_1/\partial x_1)$ equation written in the form $\sigma = f(\epsilon, \epsilon_{\mathrm{c}})$ for unloading from a maximum strain ϵ_{c}. The first-time loading curve with changing damage is $\sigma = f(\epsilon, \epsilon)$, where $\epsilon_{\mathrm{c}} = \epsilon$ is both the maximum strain and the current strain. A point on the stress-strain curve for loading $\sigma = f(\epsilon, \epsilon)$ is also an end point on an unloading or reloading curve $\sigma = f(\epsilon, \epsilon_{\mathrm{c}})$ at $\epsilon_{\mathrm{c}} = \epsilon$.

A potential Φ^D exists during a damaging process, where

$$\sigma_{ij}^R = \partial\Phi^D/\partial\left(u_{i,j}^R\right) \tag{A.3}$$

because

$$\partial\sigma_{ij}^R/\partial\left(u_{k,l}^R\right) = \partial\sigma_{kl}^R/\partial\left(u_{i,j}^R\right). \tag{A.4}$$

Equation (A.4) is easily verified for the stresses in (A.2); in evaluating the derivatives of stress, one must first set $F_{cn} = F_n$ and then differentiate both arguments of each Φ_n. It can also be shown that if at least one of the functions Φ_n were to depend on more than one damage parameter, (A.4) would not necessarily hold. In order to fully define the stresses by (3) in Section 2, we write $\Phi = \Phi^C$ when the damage is constant, $\Phi = \Phi^D$ for a damaging process, and $\Phi = \Phi^C = \Phi^D$ at the transition between the two types of processes.

As an aid in constructing Φ^D from (A.2) and (A.3) and the transition continuity condition, and in providing a physical interpretation of this damage theory, let us rewrite Φ^C in a different but equally general form. Specifically, eliminate Φ_n ($n = 1, \ldots, N$) from (A.1) in favor of new functions P_n and h_n, where

$$\Phi_n = P_n(F_n, F_{cn}) + \int_0^{F_{cn}} h_n(F_n)\,dF_n \tag{A.5}$$

and

$$P_n(F_n, F_n) = 0. \tag{A.6}$$

Notice that (A.6) implies $P_n(F_{cn}, F_{cn}) = 0$, and thus the integral in (A.5) is equal to Φ_n at the transition point, $F_n = F_{cn}$. The potential for the constant damage process may be written in the form,

$$\Phi^C = \Phi_c^D + \sum_{n=1}^{N} P_n(F_n, F_{cn}) \tag{A.7}$$

where

$$\Phi_c^D \equiv \Phi_0 + \sum_{n=1}^{N} \int_0^{F_{cn}} h_n(F_n)\,dF_n. \tag{A.8}$$

The stresses for constant damage are

$$\sigma_{ij}^R = \frac{\partial\Phi_0}{\partial\left(u_{i,j}^R\right)} + \sum_{n=1}^{N} \frac{\partial P_n}{\partial F_n}\frac{\partial F_n}{\partial\left(u_{i,j}^R\right)}. \tag{A.9}$$

Requirements of stress and potential continuity at the transition point, $F_n = F_{cn}$, together with (A.3), yield for the damaging process,

$$\Phi^D = \Phi_0 + \sum_{n=1}^{N} \int_0^{F_n} h_n(F_n')\,dF_n' \tag{A.10}$$

and

$$\sigma_{ij}^R = \frac{\partial\Phi_0}{\partial\left(u_{i,j}^R\right)} + \sum_{n=1}^{N} h_n(F_n)\frac{\partial F_n}{\partial\left(u_{i,j}^R\right)}. \tag{A.11}$$

where

$$h_n(F_n) = \partial P_n(F_n, F_{cn})/\partial F_n \quad \text{when} \quad F_{cn} = F_n. \tag{A.12}$$

Observe that $\Phi_c^D = \Phi^D$ at $F_n = F_{cn}$. Equations (A.6)-(A.12) constitute the damage theory which will be used in the remainder of the Appendix. In using (3) in Section 2 with the damage theory, it should be kept in mind that $\Phi = \Phi^C$ for constant damage, $\Phi = \Phi^D$ for a damaging process, and that stresses are given explicitly by (A.9) and (A.11).

Let us next consider the relationship of Φ^D and Φ^C to mechanical work and dissipation. Without body forces, the mechanical work input per unit initial volume for the reference problem in any given time interval $t_a \le t \le t_b$ is

$$W_{in}^R(t_a, t_b) = \int_{t_a}^{t_b}\left[\sigma_{ij}^R\partial\left(u_{i,j}^R\right)/\partial t\right]dt \tag{A.13}$$

which may be readily established by means of the divergence theorem. Take $t_a = 0$ and assume the material is initially in its undeformed state ($u_{i,j}^R = 0$) and that it does not age during the period 0 to t_b (i.e. Φ depends on time only through $u_{i,j}^R$). Without loss in physical generality, we may set $\Phi_0 = \Phi^D = 0$ at $t = 0$. Consider next an arbitrary number of intervals of damaging and constant damage processes, starting with a damaging process.

Substituting (3) into (A.13) and using continuity in Φ at the transition point between each process,

$$W_{in}^{R}(0, t_b) = \Phi^{D}(t_b) \tag{A.14}$$

when t_b falls within a damaging process, and

$$W_{in}^{R}(0, t_b) = \Phi^{C}(t_b) \tag{A.15}$$

when t_b falls within a constant damage process. Thus, for nonaging elastic materials with damage, Φ^D and Φ^C have a very simple physical meaning. Notice that if $\sigma_{ij}^{R}(t_b) = 0$ for a period of time during a constant damage process, (A.9) gives implicitly the residual values of $u_{i,j}^{R}$. During this period one can think of Φ as the mechanical work "dissipated" due to damage (in the sense that it is the net work input for one or more cycles of loading and unloading). If healing occurs during "damaging processes", the work input could be negative. For uniaxial stress-strain behavior, one may view $\Phi^{D}(t_b)$ as the area under a tensile stress-strain curve for loading, and $\Phi^{C}(t_b)$ as this area less that under the curve for unloading.

Pursuing further the physical significance of the damage theory, we find that a special microcracking case in [14, (154)] may be obtained from the present theory by setting

$$\sigma_{ij}^{R} = \sigma_{ij}, \quad N = 1, \quad F_{c1} = F_m, \quad \Phi_0 = F_1,$$

$$P_1 = -g(F_m)(F_1 - F_m), \quad g(0) = 0. \tag{A.16}$$

The damage parameter F_m is the maximum value of F_1, considering the entire deformation history up to the current time. Equation (A.12) yields $h_1(F_1) = -g(F_1)$. Also, we find

$$\Phi^{C} = [1 - g(F_m)][F_1 - F_m] + \int_0^{F_m} [1 - g(F_1)]\,dF_1 \tag{A.17}$$

and

$$\Phi^{D} = \int_0^{F_1} [1 - g(F_1')]\,dF_1'. \tag{A.18}$$

The stresses for a constant damage process are

$$\sigma_{ij} = [1 - g(F_m)]\partial F_1 / \partial(u_{i,j}^{R}). \tag{A.19}$$

For a damaging process set $F_m = F_1$ in (A.19). The function $g(F_1)$ reflects the softening effect of microcracks: for no damage $g = 0$, and for complete damage (uniform failure) $g = 1$. Observe from (A.19) that F_1 is the pseudo strain energy density for an undamaged material. It should also be added that g may vanish over an F_1 range, $0 \leq F_1 \leq F_D$, say. In this case, the "damaging process" would not actually produce damage until the energy F_D is exceeded. According to (A.17) and (A.18), $\Phi^C = \Phi^D = F_1$ for $0 \leq F_1 \leq F_D$, as expected.

A damage parameter which is more general than F_m appears in [14,15]. It is derived from viscoelastic crack growth theory, and may be written in the form of a so-called Lebesgue norm,

$$L_p \equiv \left[\int_0^t F_1^p\,dt\right]^{1/p}. \tag{A.20}$$

If $p = \infty$, (A.20) reduces to $L_p = F_m$; this case leads to the previous theory, (A.17)-(A.19). On the other hand, if p is not infinite but is at least moderately large ($p \geq 4$), and if the deformation history over a period $0 \leq t \leq t_m$ is one in which $F_m = F_1$, then [15],

$$L_p = AF_1 t^{1/p} \tag{A.21}$$

where A is essentially constant. If (A.21) applies up to $t = t_m$, and $F_1 < F_m$ for $t > t_m$, then

$$L_p = AF_m t_m^{1/p} \tag{A.22}$$

at least for a limited period of time beyond t_m. The damage model for which (A.21) and (A.22) apply may be used to generalize (A.17)-(A.19); viz., replace $g(F_m)$ with $g(F_m t_m^{1/p})$ and $g(F_1)$ with $g(F_1 t^{1/p})$. Hence, microcracking for which p is finite leads to an "aging" elastic material with damage.

The J_v integral

By dividing the continuum into regions of varying damage (i.e. where a damaging process exists) and constant damage, we may easily extend the theory in the body of the paper to allow for damage if the displacement field is sufficiently smooth. In effect, the material may be treated as nonhomogeneous whether the nonhomogeneity is intrinsic or is due to damage. As justification for this extension, consider first the integral $\mathcal{A}$, (8). We will allow for explicit dependence on x_2, x_3, and t in the potentials Φ_0 and P_n in (A.7) and (A.8) (besides dependence on $u_{i,j}^{R}$); but dependence on x_1, either explicitly or in F_{cn}, is excluded.

At any given time, let $S \equiv S_c$ enclose a region of the body undergoing a constant damage process. Clearly $\mathcal{J} = 0$ if Φ^C is used for Φ. If, for example, we were to use Φ^C from the special microcracking model (A.17), it would be necessary for the maximum energy F_m to be independent of x_1, although F_m could vary with x_2 (distance from the local crack plane) and x_3. Now, let $S \equiv S_D$ enclose an adjacent region undergoing a damaging process. Here, $F_{cn} = F_n$, and thus $\mathcal{J} = 0$ if Φ^D is used for Φ, even though F_{cn} may vary with x_1; this dependence is through $F_n = F_n(u_{i,j}^R)$ and therefore it causes no problem. Next, take $S = S_c + S_D$, and consider the interface where S_c and S_D are adjoining surfaces. The contribution to $\mathcal{J}$ along the interface from both S_c and S_D vanishes if $\partial u_i^R/\partial x_1$, Φ, and Φ_F are continuous across the interface; this follows from the fact that n_1 and T_i^R are continuous in magnitude at the interface but have opposite signs on S_c and S_D. Consequently, if the transition between a damaging process and a constant damage process is sufficiently smooth (8) and (10) hold, and surface-independence of J_x, (11), and path independence of J_x, (12), exist, as an obvious generalization. S may surround an arbitrary number of connected zones with both types of processes.

It is important to recall that $\partial F_{cn}/\partial x_1 = 0$ is required in each constant damage process zone. For example, suppose the body is loaded and a damaging process zone with nonuniform damage is produced. Upon partial unloading, this zone may become a constant (with respect to time) damage process zone, but $\partial F_{cn}/\partial x_1$ and therefore $\mathcal{J}$ for this zone would not in general vanish.

As an illustration of the use of this theory, consider the crack growth problem of Fig. 5 treated in the body of the paper. Locally steady-state crack propagation is assumed. We suppose that a given material element in the process zone b undergoes a damaging process as the crack tip P approaches it, which changes to a constant damage process by the time the left end of the failure zone, $\xi = \alpha$, arrives. Now, by definition, the steady-state condition is one in which each element in the constant damage part of the process zone has damage parameters which are independent of x_1; e.g., for the simple microcracking model $\partial F_m/\partial x_1 = 0$. Path independence in the process zone b then permits us to evaluate J_{fa} from J_{cb} (cf. (61)) using the contour C_1 in Fig. 5. The result for J_{cb} is in (68), where I_α is the line integral of $-\Phi_b$ at $\xi = \alpha$, (70). The potential Φ_b is actually Φ_c^f if a constant damage process exists at $\xi = \alpha$ above and below the failure zone. In view of (A.15), the integral, $-I_\alpha$, is the net work input to the process zone per unit volume integrated from the bottom to the top of the process zone. If there is no damage in the process zone ($P_n = 0$) and the pseudo strain energy density vanishes at $\xi = \alpha$, then $I_\alpha = 0$. However, dissipation would still exist for a viscoelastic material; it is reflected in the speed dependent creep compliances which appear in (71).

Energy release rate

Equation (17) applies with damage, even if the homogeneity condition in x_1 needed for J_x is not satisfied. This generalization may be shown by retracing the proof without damage, but using Φ^C and Φ^D for Φ where appropriate. Only the virtual work (13) needs to be examined as the subsequent steps, (14)–(16), are unaffected. Self-similar, virtual crack advancement is imposed through application of appropriate surface tractions to derive (17), even though in an actual crack growth process this type of advancement may not occur.

The validity of (13) may be established using the same procedure as for (8) with damage. Namely, divide the body into constant damage and damaging process regions. Inasmuch as a change in the displacement field occurs due to δa, thin layers of thickness on the order of δa have to be excluded; these are the layers in which the type of process changes during the crack advancement. However, if Φ and δu_i are continuous in x_2, the work and pseudo strain energy associated with these layers is of order $(\delta a)^2$, i.e. thickness $\times\ \delta u_i$, and thus the layers do not affect the result in the limit $\delta a \to 0$; other contributions to (13), including δW^R in (16), are of order δa.

Generalization of the damage model

So far we have considered only the case in which the potential for constant damage is given by (A.7) and all of the damage parameters satisfy $F_{cn} = F_n$ or else all are constant. The model may be easily generalized by adding one or more similar groups of terms to Φ^C, with each group possibly representing a different physical mechanism. The regions of constant and varying damage for one group need not be at the same locations as those for another group.

A constant damage potential which has a direct effect on residual stresses due to damage is

$$\Phi^C = \Phi_{rc} + \left(u_{i,j}^R - u_{i,jc}^R\right)\left(\frac{\partial \Phi_r}{\partial u_{i,j}^R}\right)_c \tag{A.23}$$

where $\Phi_r = \Phi_r(u_{i,j}^R)$ and the subscript c indicates that $u_{i,j}^R$ is constant during a constant damage process. The stresses corresponding to this potential are constant,

$$\sigma_{ij} = \left(\frac{\partial \Phi_r}{\partial u_{i,j}^R}\right)_c \tag{A.2}$$

For a damaging process $u^R_{i,jc} = u^R_{i,j}$, and a potential exists whose value is $\Phi^D = \Phi_r(u^R_{i,j})$; the associated stresses are given by (A.24), but without the subscript c. These potentials may be added to (A.7) and (A.10) to generalize the damage theory. More than one potential Φ_r may be used, with each depending on different combinations of the displacement derivatives. As one example, we obtain the Hencky deformation theory [26] with linear elastic unloading if (A.23) is added to only Φ_0, where Φ_0 is taken as the strain energy density for an isotropic linear elastic material, we use $u^R_i = u_i$ and linear strain-displacement equations, and assume Φ_r depends on displacement derivatives through the so-called effective strain invariant; for loading in a plastic state, $\Phi^D = \Phi_0 + \Phi_r$. Addition of (A.23) and Φ_r to potentials for the special microcracking model, (A.17) and (A.18) respectively, enables one to account for an effect of microcracking on residual stresses.

The results in the Appendix concerning the interpretation of Φ^D and Φ^C as mechanical work, (A.14) and (A.15), as well as the J_v integral and energy release rate, are valid with these extensions of the damage model. However, each group in the total potential Φ has to be considered separately since, at any given time and location, some may be for damaging processes and others for constant damage processes.

Résumé

On développe des méthodes d'analyse des déformations et de rupture quasi statiques pour une classe de milieux visco-élastiques non linéaires et on illustre des applications types de ces méthodes. Le choix de la classe est dicté par le comportement rhéologique réel de matériaux monolitiques ou composites, ainsi que par la nécessité de simplifier l'approche pour comprendre l'effet des paramètres de base du matériau et du continuum sur leur comportement vis-à-vis de la croissance de la fissure. On discute en premier lieu la pertinence des théories de l'intégrale J et du taux de relaxation d'énergie, dans le cas de milieux élastiques non linéaires. On établit ensuite des équations visco-élastiques non linéaires et on développe les principes de correspondance qui permettent de mettre en place une relation simple entre les état mécaniques correspondant à des milieux élastiques et à des milieux visco-élastiques.

On tire des principes une base pour étendre la théorie de l'intégrale J à la croissance de fissures dans les matériaux visco-élastiques. L'accent est placé sur la prédiction du travail mécanique susceptible d'amorcer et d'entretenir la croissance d'une fissure à l'extrémité de celle-ci. Quelques exemples montrent comment le comportement à la croissance est influencé par les propriétés visco-élastiques et par l'intégrale J.

L'étude couvre le cas d'une fissure dans une couche mince présentant des propriétés visco-élastiques distinctes de celles du substrat. En annexe, on présente une théorie apparemment originale sur les matériaux élastiques et visco-élastiques comportant des microstructures évolutives et on indique les conditions selon lesquelles la théorie de la rupture discutée dans le mémoire est applicable.

Texas A&M University
Mechanics & Materials Center
Report MM 5034-85-8
May, 1985

DEFORMATION AND FRACTURE CHARACTERIZATION OF INELASTIC NONLINEAR MATERIALS USING POTENTIALS*

by
R.A. Schapery
Department of Civil Engineering
Texas A&M University, College Station, Texas 77843

Many important results on the deformation and fracture of linear and nonlinear elastic materials have been obtained by using strain energy potentials to characterize material response. Besides serving as the basis for powerful methods of exact and approximate structural analysis, local and global strain energy functions have been used in the prediction of effective constitutive properties (or their upper and lower bounds) of multiphase media in terms of properties and geometry of the phases; included are studies of the effect of constant damage, in the form of small distributed cracks and voids, on the global stress-strain behavior of monolithic and composite materials [e.g., 1,2].

Strain energy concepts are used widely in fracture mechanics [3]. For elastic materials, the mechanical work available at a crack tip for producing crack growth is equal to the decrease in potential energy (consisting of global strain energy and the boundary work potential), and this relationship has resulted in remarkably successful investigations of fracture of rubber in its nonlinear range of behavior [4], as well as linear elastic materials.

In this talk we discuss inelastic behavior, and consider the question of whether or not potentials which are analogous to strain energy may be used to characterize deformation and fracture. The ideas are illustrated using data on polymeric composite materials. First, elastic materials, but with timewise constant and changing distributed "microdamage", are discussed. Then viscoelastic behavior and macrocrack growth are considered briefly.

Theory: The concept of a potential for elastic materials with damage may be introduced through the uniaxial stress-strain curve in Fig. 1. Let us suppose that a previously undamaged specimen is strained monotonically until the strain is ϵ_m. The strain is then reduced, as shown in Fig. 1. Assuming that the bar is elastic and has constant damage during the unloading period, with stress σ^U, and that the maximum strain ϵ_m serves to define the amount and effect of damage, we may write

$$\sigma^U = f(\epsilon,\epsilon_m) \tag{1}$$

The maximum strain at any time equals the current strain on the loading curve, and thus

$$\sigma^L = f(\epsilon,\epsilon) \tag{2}$$

The mechanical work (per unit initial volume) during loading to an arbitrary strain is

$$\phi^L = \phi^L(\epsilon) \equiv \int_0^\epsilon \sigma^L \, d\epsilon' = \int_0^\epsilon f(\epsilon',\epsilon') d\epsilon' \tag{3}$$

where the prime denotes a dummy variable of integration. The net work input to the sample at any time during unloading is the shaded area in Fig. 1.

$$\phi^U = \phi^U(\epsilon,\epsilon_m) \equiv \phi^L(\epsilon_m) + \int_{\epsilon_m}^\epsilon \sigma^U \, d\epsilon'$$

$$= \phi^L(\epsilon_m) + \int_{\epsilon_m}^\epsilon f(\epsilon',\epsilon_m) \, d\epsilon' \tag{4}$$

Observe that during loading and unloading, respectively,

$$\sigma^L = d\phi^L/d\epsilon, \quad \sigma^U = \partial\phi^U/\partial\epsilon \tag{5}$$

It is convenient to let ϕ denote a quantity which equals ϕ^L during loading ($\epsilon_m = \epsilon$) and equals ϕ^U during unloading ($\epsilon<\epsilon_m$). Then, we may write for both loading and unloading processes,

$$\sigma = \partial\phi/\partial\epsilon \tag{6}$$

and therefore the quantity ϕ is a "work potential" which becomes the usual strain energy density when the loading and unloading curves are identical. Obviously, a work potential ϕ can always be constructed, given the uniaxial stress-strain curves, Eqs. (1) and (2).

For characterization of the multiaxial stress-strain behavior, or for other response functions which depend on more than one independent input, a work potential does not necessarily exist. However, that it can be expected to exist for some realistic situations will be discussed here. For purposes of generality, let us use as independent inputs the generalized displacements q_j (j=1,2,...J). The responses are the generalized forces Q_j, which are defined in the normal way by the condition that, for each j,

$$\delta W = Q_j \delta q_j \tag{7}$$

where δW is the virtual work input associated with the virtual displacement δq_j. Suppose, for example, we let each q_j represent an independent component of a suitably defined three-dimensional strain tensor and let δW be virtual work per unit initial volume. Then, J=6 and Eq. (7) implies the set Q_j represents the components of a stress tensor (for large or small strains). In order to characterize the behavior of laminates, one may want to identify the set q_j with the middle surface curvatures and strains. In this case, the Q_j would correspond to moments and in-plane forces per unit length.

As in the uniaxial example, we assume that when the damage is constant the body (material element, test specimen, or complete structure) is elastic in the usual sense, i.e., a strain energy function or work potential ϕ^C exists with the property that

$$Q_j = \partial\phi^C/\partial q_j \tag{8}$$

(Rather than using the terms "loading" and "unloading" we shall instead now refer to "damaging processes" and "constant damage processes", since we do not want to imply that the damage is always constant when the magnitude of one or more loads or displacements decreases with time.) The effect of damage on Q_j is assumed to be fully represented by a set of parameters F_{cn} (n=1,2,....N). Following the arguments in [5] it can be shown that a work potential ϕ^D exists during damaging processes such that

$$Q_j = \partial\phi^D/\partial q_j \tag{9}$$

where ϕ^D is a function of only the current values of q_j, if ϕ^C has the form,

$$\phi^C = \phi_o(q_j) + \sum_{n=1}^N \phi_n(F_n,F_{cn}) \tag{10}$$

where ϕ_o is the work potential without damage. The functions $F_n = F_n(q_j^o)$ are to be selected such that $F_{cn} = F_n$ during damaging processes. (To recover the uniaxial case, Eqs. (1) and (2), we set N=1 and take $F_1=q_1=\epsilon$, $F_{c1}=\epsilon_m$). It should be noted that "internal variables" are not used in this theory. Of course, one could think of the set F_{cn} as "internal parameters" which are constant during constant damage processes and which vary in such a way that $F_{cn} = F_n$ for damaging processes. For laminates, an F_n may be an invariant of ply (or ply-pair) strains, where the summation in Eq. (10) would extend over all plies.

Generalizations of this formulation are discussed in [5]. For example, at any given time some of the terms ϕ_n in Eq. (10) may be for constant damage processes while others are for damaging processes. Also, the potentials may depend explicitly on time, and thus provide for effects of aging or changing physical environments. (The theory in [5], which allows for large deformations, uses displacement gradients and Piola stresses instead of generalized displacements and

*Sponsored by the Air Force Office of Scientific Research

This research summary was prepared for publication in Polymer Preprints for the International Symposium on Non-Linear Deformation, Fracture and Fatigue of Polymeric Materials, National Meeting of the American Chemical Society, Chicago, September 1985.

forces. However, the earlier formulation, including its extension to viscoelastic behavior, carrys over fully in terms of the generalized variables used here.) Thus, as in Eq. (6), we may write

$$Q_j = \partial\phi/\partial q_j \qquad (11)$$

even if the damage parameters in some components ϕ_n are constant and others are varying in time. Also,

$$\partial Q_i/\partial q_j - \partial Q_j/\partial q_i = 0 \qquad (i,j = 1,2,\ldots J) \qquad (12)$$

except at the points of change from one process to another, considering all ϕ_n. The derivatives in Eq. (12) are, in general, discontinuous at these transition points (cf. Fig. 1) and thus Eq. (12) does not apply there; we assume, however, that the derivatives are continuous functions of displacements at all other points. Evidence of transition points may appear in experimental data as non-zero values of this difference of derivatives (for $i \neq j$) over short time intervals.

It is not necessary for the constant-damage potential to have the form in Eq. (10) for the work potential in Eq. (11) to exist. For example, a different form for ϕ^C was given in [5] which contains the deformation theory of plasticity (with elastic unloading). We may extend the present model to account explicitly for stable micro- or macrocrack growth. (Certain microcrack effects are at least implicitly contained in the ϕ discussed so far.) An important extension is obtained by adding a term which is equal to the mechanical energy required at crack tips to extend any micro- or macrocracks not already accounted for in ϕ. For example, if the energy required per unit of surface area A (projected onto the local crack plane) were constant, with value Γ, then one would add the "fracture potential" ΓA to ϕ to obtain the total potential. Without assuming the fracture energy Γ is constant or is the same for all cracks, let us suppose a fracture potential $\phi_f = \phi_f(A_k,t)$ exists, where A_k (k=1,2,...K) represents the set of all (oriented) crack surface areas needed to define the effect of all cracks not accounted for in ϕ; time t is shown to indicate that the required crack-tip work may be affected by material aging, fatigue, transient temperature, etc. The total potential is

$$\phi_T = \phi_f + \phi \qquad (13)$$

where ϕ is that in Eq. (11). The mechanical work available at the edge of the kth crack area A_k is $-\partial\phi/\partial A_k$, where $\phi=\phi(q_j,A_k)$, whether or not the damage parameters F_{cn} vary [5, p. 222]. Thus, for stable quasi-static crack growth or no growth, respectively,

$$\partial\phi_f/\partial A_k = -\partial\phi/\partial A_k \quad \text{or} \quad \partial\phi_f/\partial A_k > -\partial\phi/\partial A_k \qquad (14)$$

The first relationship is a set of equations for finding all of the corresponding A_k as functions of q_j. Using both cases in Eq. (14), it is readily shown that

$$Q_j = \partial\phi_T/\partial q_j \qquad (15)$$

with constant crack areas, and with growing cracks when the derivatives $\partial A_k/\partial q_j$ exist. All A_k for microcracks which are uniquely determined as functions of q_j by the first expression in Eq. (14) may be interpreted as damage parameters and thus included (possibly as functions of A_k) in the set F_{cn}; the fracture energy of these A_k would not be contained in ϕ_f. When multiple solutions for growing A_k exist, the displacement history is needed to be able to predict the actually occuring values. For this case and for macrocracks one could not include A_k (or functions of A_k) in the F_{cn}.

Experimental Studies: Farris [6] showed, in effect, that a particle-filled rubber, with void growth, under axial stress and confining pressure obeyed Eq. (12) (with q_1 = ε, q_2 = dilatation) for constant axial strain rates. Thus, at least in a limited study, the work potential with damage growth was established. Strain-history effects due to viscoelasticity and damage have been taken into account in more recent work [7]. We are presently studying the validity of the elastic and viscoelastic theory with damage for graphite/epoxy tube and plate specimens. In some cases there is a very significant nonlinear effect of axial strain on shear behavior, as illustrated in Fig. 2. Specimen failure often occurs by delamination, and this type of macrocrack is being analyzed using Eq. (14). Recent findings from this investigation will be described.

References

[1] Hashin, Z., "Analysis of Composite Materials - A Survey", Journal of Applied Mechanics 50 (1983) 481-505.

[2] Duva, J.M. and Hutchinson, J.W., "Constitutive Potentials for Dilutely Voided Nonlinear Materials," Mechanics of Materials 3 (1984) 41-54.

[3] Broek, D., Elementary Engineering Fracture Mechanics, Third Ed., Martinus Nijhoff Publishers (1982).

[4] Lake, G.J., "Aspects of Fatigue and Fracture of Rubber," In: Progress of Rubber Technology, Applied Science Publishers Ltd (1983) 89-143.

[5] Schapery, R.A., "Correspondence Principles and a Generalized J Integral for Large Deformation and Fracture Analysis of Viscoelastic Media," International Journal of Fracture 25 (1984) 195-223.

[6] Farris, R.J., "The Character of the Stress-Strain Function for Highly Filled Elastomers," Trans. Society of Rheology 12:2 (1968) 303-314.

[7] Schapery, R.A., "Models for Damage Growth and Fracture in Nonlinear Viscoelastic Particulate Composites," Proc. Ninth U.S. National Congress of Applied Mechanics, ASME Book No. H00228 (1982) 237-245.

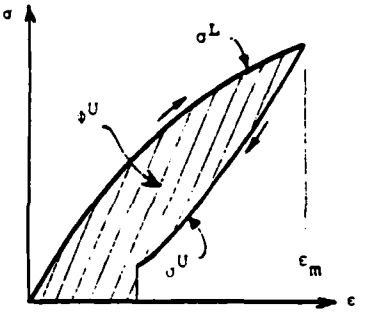

Figure 1. Uniaxial stress-strain curve for elastic material with increasing damage during loading (σ^L) and constant damage during unloading (σ^U).

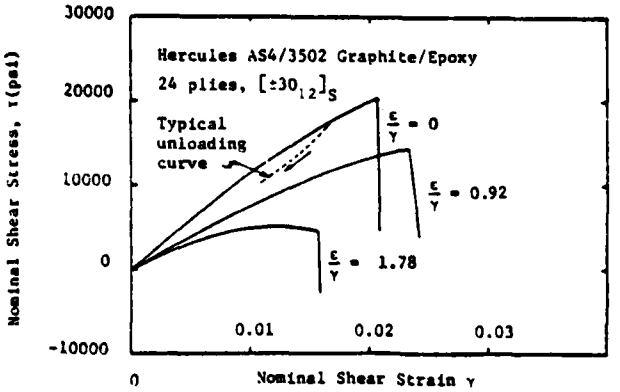

Figure 2. Shear stress-strain curves with changing axial strain ε, from axial-torsion tests of flat rectangular laminates of fiber-reinforced resin.

MATRIX CONTROLLED DEFORMATION AND FRACTURE ANALYSIS OF FIBROUS COMPOSITES*

R.A. Schapery
with Graduate Students
J.R. Weatherby
R.D. Tonda

Mechanics & Materials Center
Texas A&M University
College Station, TX 77843

ABSTRACT

Methods of quasi-static deformation and fracture analysis have been developed for nonlinear elastic, viscous, and viscoelastic materials with distributed damage [1]. The crack growth theory, which uses a generalized J integral that allows for viscoelasticity and distributed microscale damage, is not much more involved than that of nonlinear elasticity or special cases of linear viscoelasticity. This simplicity, compared to what one may expect, is a direct result of the particular type of constitutive equations and mechanical variables selected to characterize rheological behavior. Considering elastic materials with distributed damage, for example, the constitutive theory is expressed in terms of one strain energy-like potential for loading and another for unloading. The research activity is presently in the early stages of an investigation of the applicability of the theory to deformation and fracture of fiber-reinforced plastics. It is anticipated that additional information on its applicability will come from other AFOSR-sponsored projects at Texas A&M under the direction of Professors Allen, Bradley, Kinra, and Weitsman.

In this presentation we illustrate some features of the theory for elastic composite materials with damage and discuss current research activities. One important question is concerned with whether or not strain energy-like potentials actually exist; it has been addressed theoretically in [1] with encouraging results. Some examples of real nonlinear material behavior which can be characterized in this manner are given in this presentation, and then our experimental program to study this question for nonlinear behavior of unidirectional laminates is described. Another portion of the work is concerned with application of the theory to fracture characterization and analysis, assuming the requisite potentials exist. In this case the finite element method is being used to predict crack initiation and growth in materials with large-scale distributed damage, first for initially isotropic and homogeneous media and then for composites (i.e., delamination initiation and growth). A few years ago we employed linear elastic fracture mechanics in an investigation of the fracture behavior of a randomly oriented glass fiber reinforced plastic, SMC-R50 [2]. The data on this nonlinear material are reinterpreted here using J integral theory in order to further illustrate its use. Application of J integral theory to delamination growth when large-scale distributed damage exists is under study on Professor Bradley's project.

REFERENCES

1. R.A. Schapery, "Correspondence Principles and a Generalized J Integral for Large Deformation and Fracture Analysis of Viscoelastic Media," Int. J. Fracture, July 1984.

2. R.M. Alexander, R.A. Schapery, K.L. Jerina, and B.A. Sanders, "Fracture Characterization of a Random Fiber Composite Material," in Short Fiber Reinforced Composite Materials, ASTM STP 772, B.A. Sanders, Ed., pp. 208-224, 1982.

*Presented at the Tenth Annual Mechanics of Composites Review Conference, Dayton Ohio, October 1984.

This research is sponsored by the Air Force Office of Scientific Research under grant AFOSR-84-0068.

CONSTITUTIVE THEORY USING POTENTIALS FOR MATERIALS WITH DAMAGE

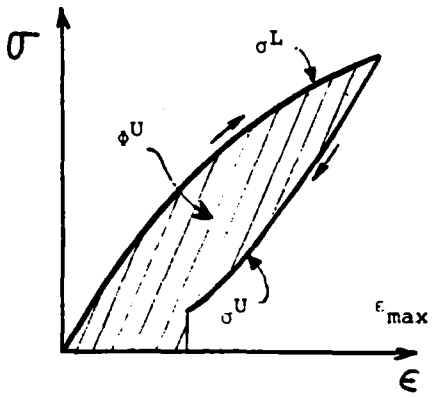

Uniaxial Loading

$$\sigma^L = f(\epsilon,\epsilon) = \frac{d\phi^L}{d\epsilon}$$

Unloading

$$\sigma^U = f(\epsilon, \epsilon_{max}) = \frac{\partial \phi^U}{\partial \epsilon}$$

Multiaxial Loading

$$\sigma^L_{ij} = \partial\phi^L/\partial\epsilon_{ij}$$

Unloading

$$\sigma^U_{ij} = \partial\phi^U/\partial\epsilon_{ij}$$

FEATURES

- CONVENIENT FORMULATION FOR FRACTURE APPLICATIONS
- DAMAGE PARAMETERS (E.G. ϵ_{max}) ARE EXPRESSED IN TERMS OF STRAIN HISTORY AND MAY BE RELATED TO PHYSICS OF DAMAGE PROCESS
- POTENTIALS ANALOGOUS TO STRAIN ENERGY DENSITY ARE USED FOR LOADING (ϕ^L) AND UNLOADING (ϕ^U)
- ALLOWS FOR TEMPERATURE AND MOISTURE INDUCED STRESSES
- VISCOELASTIC EFFECTS ARE INTRODUCED BY USING "PSEUDO DISPLACEMENTS" IN PLACE OF DISPLACEMENTS

APPLICATIONS

- EXISTENCE OF POTENTIALS SHOWN IN THE SPECIAL CASES OF PARTICLE-REINFORCED RUBBER, ELASTO-PLASTIC BEHAVIOR OF METALS AND SECONDARY AND TERTIARY CREEP OF METALS
- USE FOR FIBER-REINFORCED PLASTICS IS UNDER STUDY

CONSTITUTIVE EQUATION EXAMPLE

A SPECIAL PARTICULATE COMPOSITE WITH MICROCRACKING

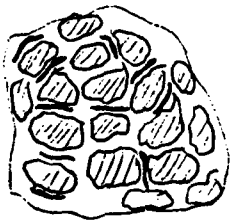

$$\phi^L = \int_o^W \left[1 - g(W')\right] dW'$$

$$\phi^U = \left[1 - g(W_M)\right]\left[W - W_M\right] + \int_o^{W_M} \left[1 - g(W)\right] dW$$

where W = STRAIN ENERGY DENSITY WITHOUT DAMAGE ($g = 0$)

W_M = MAXIMUM W

- NOTE THAT $\phi^L = \phi^U$ WHEN $W = W_M$
- STRESSES ARE

$$\sigma_{ij}^L = \frac{\partial \phi^L}{\partial \varepsilon_{ij}} = \left[1 - g(W)\right] \frac{\partial W}{\partial \varepsilon_{ij}}$$

$$\sigma_{ij}^U = \frac{\partial \phi^U}{\partial \varepsilon_{ij}} = \left[1 - g(W_M)\right] \frac{\partial W}{\partial \varepsilon_{ij}}$$

GIVES REDUCED STIFFNESS WHEN $0 < g \leq 1$

APPROACH FOR UNIDIRECTIONAL PLY CHARACTERIZATION

CONSIDER A UNI-AXIALLY LOADED, OFF-AXIS, UNIDIRECTIONAL COMPOSITE TENSILE SPECIMEN. THE STRESSES IN THE PRINCIPAL MATERIAL DIRECTIONS ARE WRITTEN IN TERMS OF THE STRAINS IN THOSE DIRECTIONS AS (NEGLECTING EFFECTS OF END CONSTRAINT):

$$\sigma_1 = \sigma_1(\epsilon_1, \epsilon_2, \gamma_{12}),$$

$$\sigma_2 = \sigma_2(\epsilon_1, \epsilon_2, \gamma_{12}),$$

$$\tau_{12} = \tau_{12}(\epsilon_1, \epsilon_2, \gamma_{12}).$$

IF A POTENTIAL ϕ IS TO EXIST, SUCH THAT

$$\sigma_1 = \partial\phi/\partial\epsilon_1, \quad \sigma_2 = \partial\phi/\partial\epsilon_2, \quad \tau_{12} = \partial\phi/\partial\gamma_{12}$$

IT IS NECESSARY THAT, FOR EXAMPLE,

$$\left.\frac{\partial\sigma_2}{\partial\gamma_{12}}\right|_{\epsilon_1,\epsilon_2 = \text{CONST.}} = \left.\frac{\partial\tau_{12}}{\partial\epsilon_2}\right|_{\epsilon_1,\ \gamma_{12} = \text{CONST.}}$$

- PERFORM TESTS ON AS4/3502 MATERIAL USING OFF-AXIS SPECIMENS.

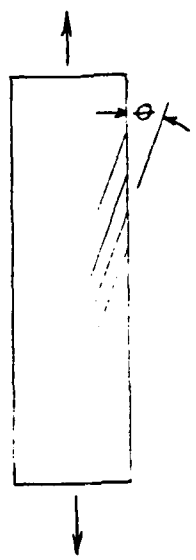

θ = FIBER ANGLE

BY VARYING θ, THE NECESSARY DATA CAN BE DEVELOPED TO EVALUATE THE CROSS-DERIVATIVES AND DETERMINE THE EXISTENCE OF ϕ.

THESE DATA ALSO CAN BE USED TO DEVELOP THE POTENTIAL ϕ ITSELF.

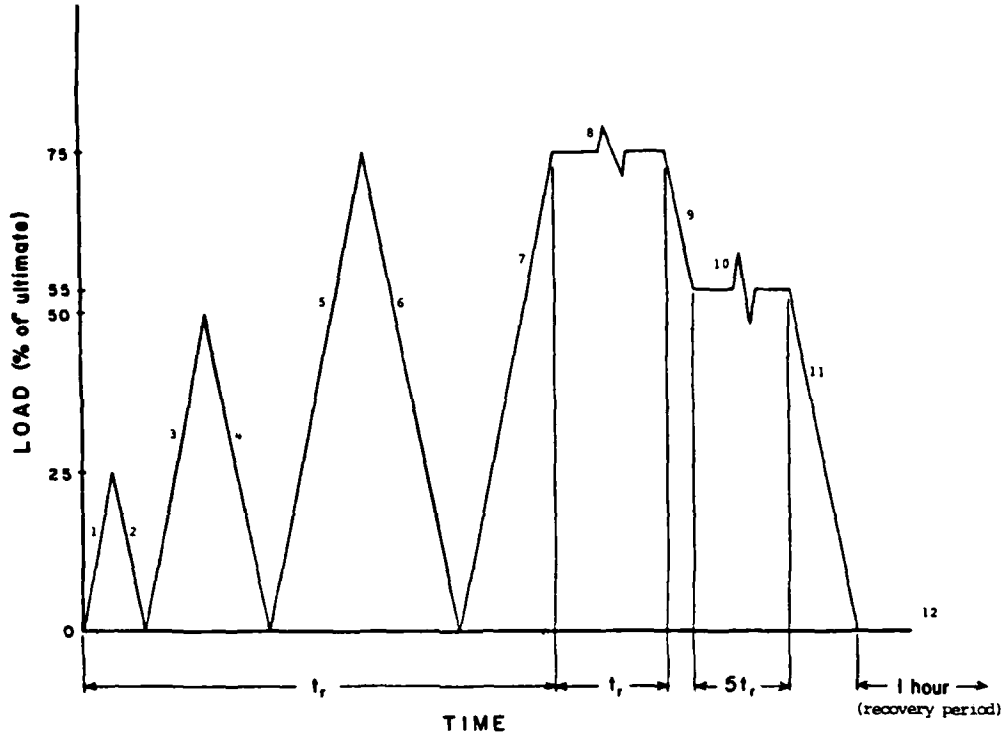

Figure 1. Load-time history used in 30° off-axis tests. (tr = 210 sec.)

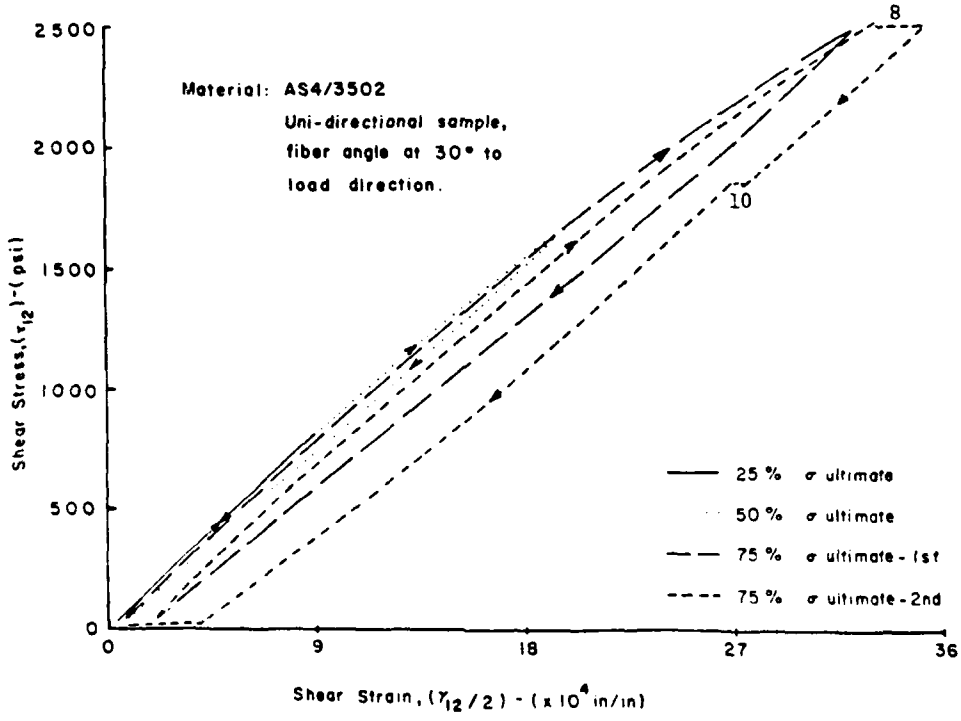

Figure 2. Shear stress versus shear strain from test in Figure 1.

FRACTURE EXAMPLE

- FRACTURE OF EDGE-NOTCHED COUPONS OF A SHORT FIBER COMPOSITE, SMC-R50

LOAD-DISPLACEMENT RELATION:

$$P = Cu^n , \quad n = 0.78$$

WHERE

$$C = C(a) , \quad a = \text{depth of edge notch}$$

LOADING POTENTIAL ("STRAIN ENERGY"):

$$\Phi = \int_o^u Pdu = Cu^{(n+1)}/(n+1)$$

J INTEGRAL ("ENERGY RELEASE RATE"):

$$J = -\frac{1}{B}\frac{\partial \Phi}{\partial a} = -\frac{u^{n+1}}{(n+1)B}\frac{dC}{da}$$

SET $J = J_c$ AND SOLVE FOR FRACTURE DISPLACEMENT u_f AND THEN FRACTURE STRESS σ_f.

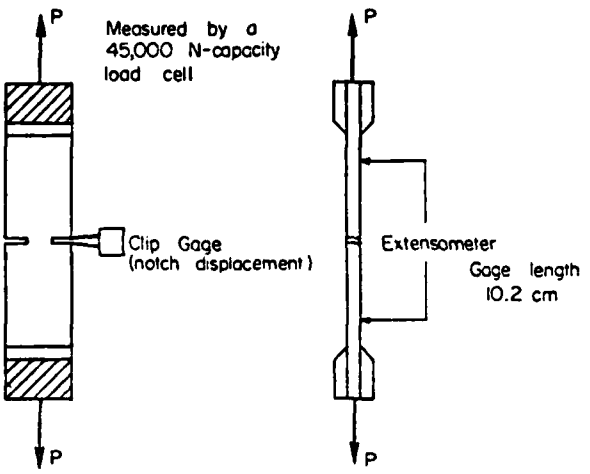

Figure 3. Double edge notch specimen with measured parameters indicated. (SMC-R50)

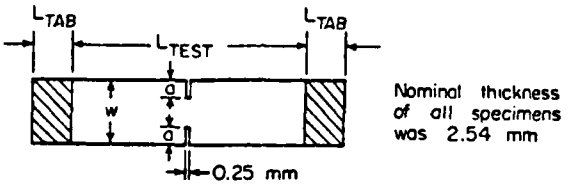

Figure 4. Double edge notch specimen geometry. (SMC-R50)

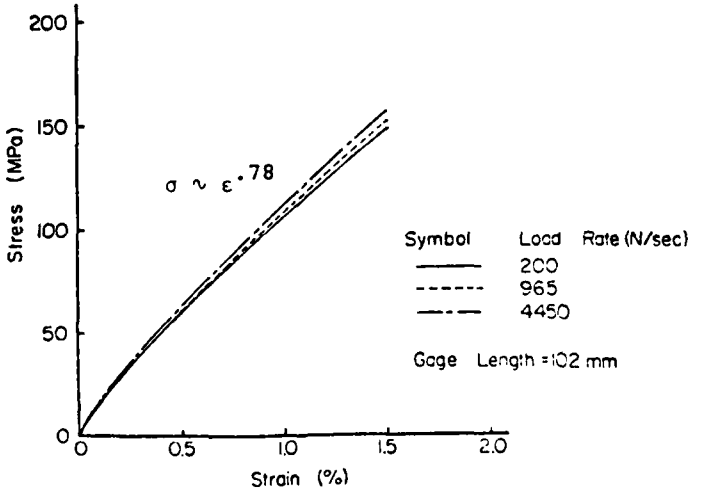

Figure 5. Stress-strain curves based on load-displacement data for 25.4 mm-wide unnotched tensile specimens. (SMC-P50)

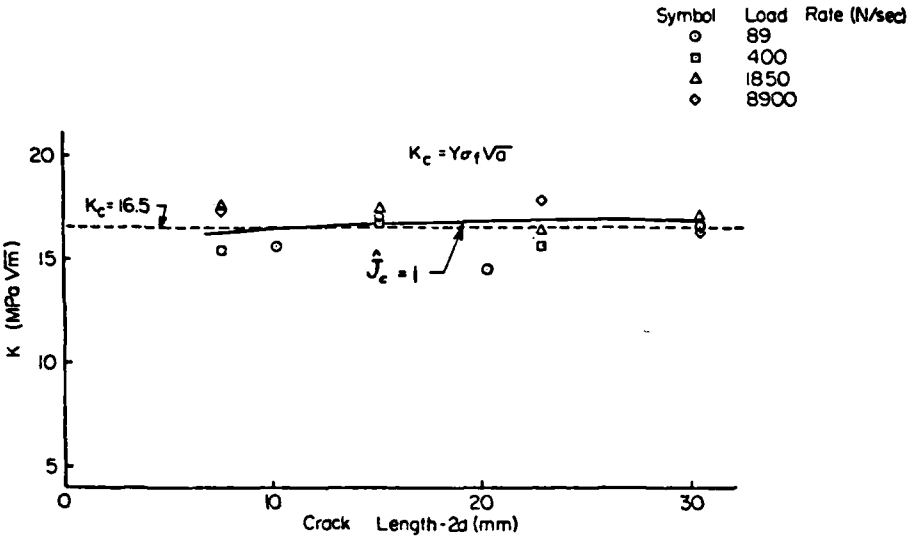

Figure 6. Critical stress intensity factor for the 50.8 mm-wide specimens. (SMC-R50)

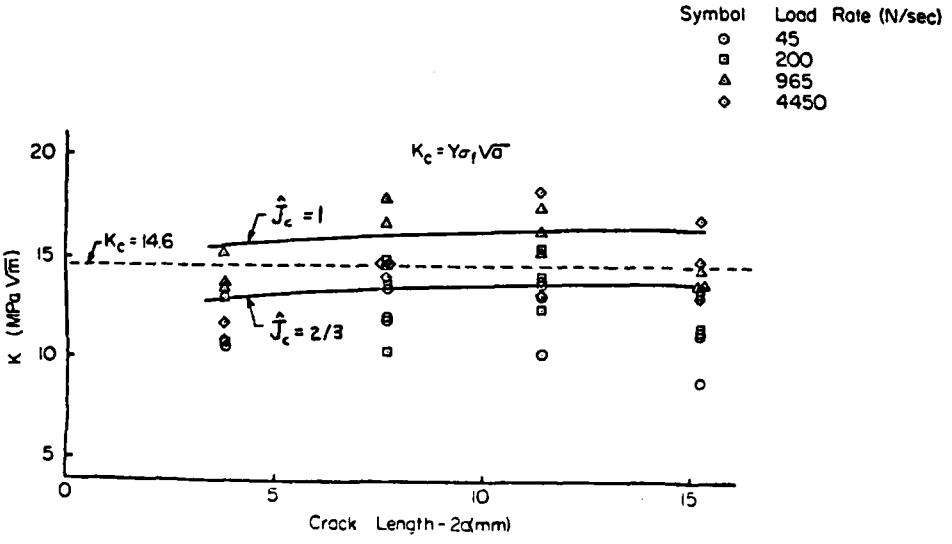

Figure 7. Critical stress intensity factor for the 25.4 mm-wide specimens. (SMC-R50)

ANALYSIS OF CRACK GROWTH IN DAMAGED MEDIA USING A GENERALIZED J INTEGRAL

- ANALYZE THE INITIATION AND PROPAGATION OF A CRACK IN A MATERIAL WITH DAMAGE THROUGH THE USE OF A FAILURE ZONE CRACK TIP MODEL AND THE GENERALIZED J INTEGRAL.

INITIALLY, THE ISOTROPIC MATERIAL MODEL OF J_2 DEFORMATION THEORY OF PLASTICITY, MODIFIED BY ELASTIC UNLOADING, IS BEING USED:

$$\sigma'_{ij} = 2G_d(\tau_s)\epsilon'_{ij}, \quad \text{for} \quad \tau_s = (\tau_s)_{max}$$

$$\sigma'_{ij} = \sigma'^{m}_{ij} = 2G(\epsilon'_{ij} - \epsilon'^{m}_{ij}), \quad \text{for} \quad \tau_s < (\tau_s)_{max}$$

$$\sigma_{kk} = 3K\epsilon_{kk}$$

WHERE: $\sigma'_{kj} = \sigma_{ij} - \frac{1}{3}\delta_{ij}\sigma_{kk}$

$$\tau_s = (\tfrac{1}{2}\sigma'_{ij}\sigma'_{ij})^{1/2}$$

EXTENSION TO ORTHOTROPIC COMPOSITES WITH DAMAGE TO FOLLOW

- FAILURE ZONE MODEL FOR THE CRACK TIP:

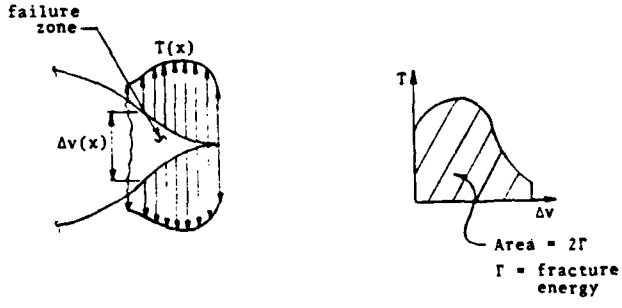

- THE J INTEGRAL IS USED TO OBTAIN INFORMATION ABOUT WORK INPUT TO THE FAILURE ZONE FROM REMOTE FIELD QUANTITIES:

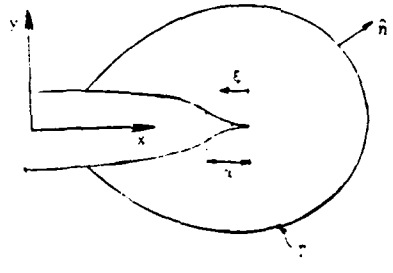

$$J = \int_\Gamma \left(\mathcal{W} n_1 - T_i \frac{\partial u_i}{\partial x}\right) ds$$

$$J_f = \int_0^a T_i \frac{\partial \Delta u_i}{\partial \xi}\, d\xi$$

$$J = J_f$$

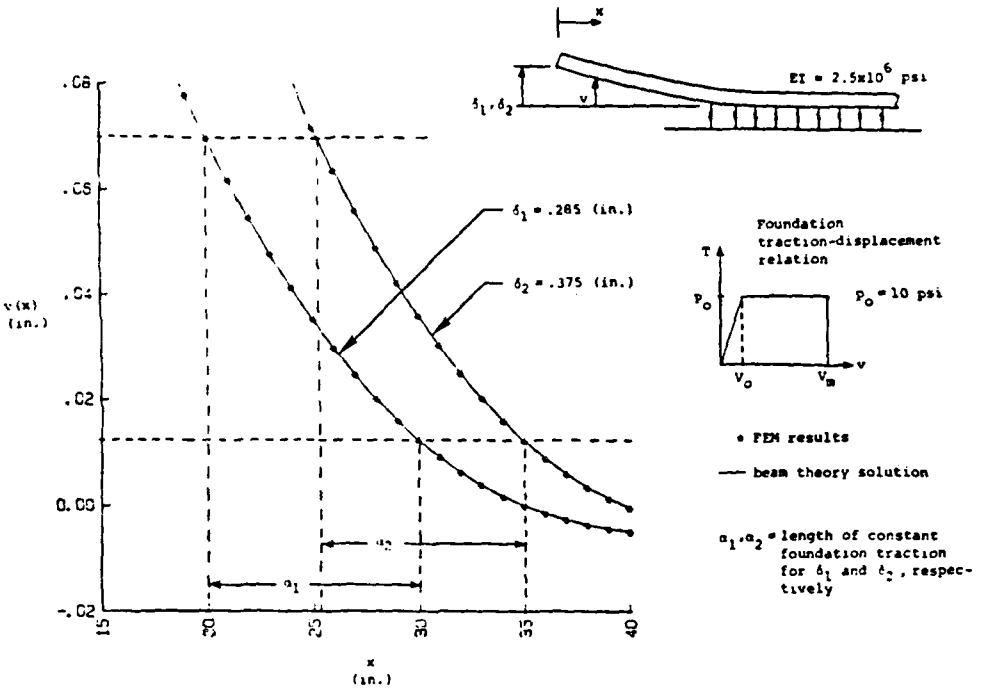

Figure 8. Deflections in a cantilever supported by an elastic-plastic foundation in which the tractions vanish above a critical displacement.

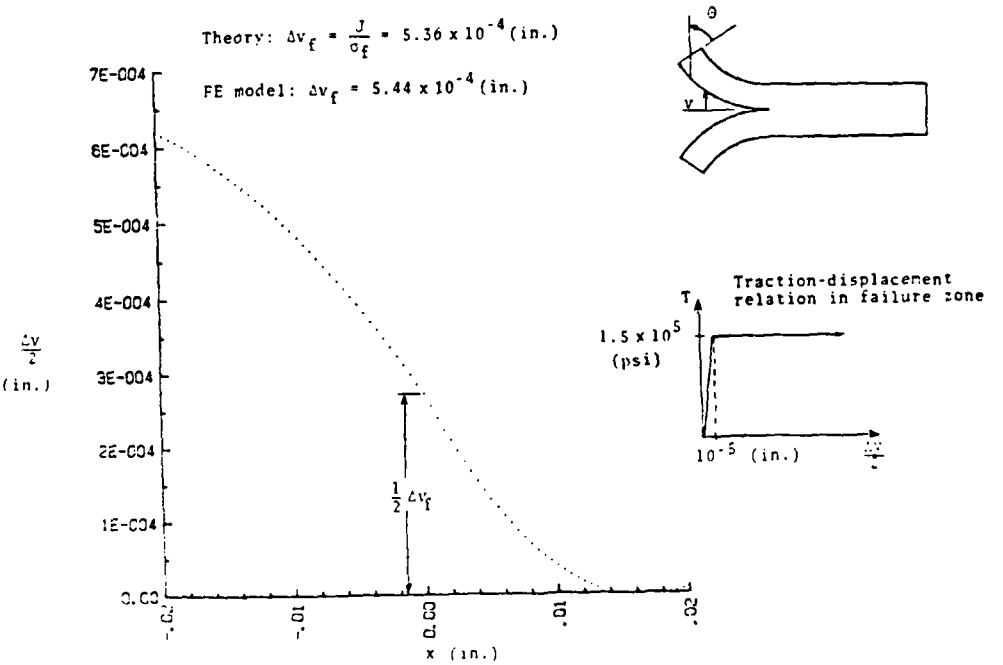

Figure 9. Crack opening displacement profile for thick, nonlinear bend specimen.

END
FILMED
4-86
DTIC